MEASUREMENT OF ADSORPTION STAY-TIMES OF SEVERAL ATMOSPHERIC GASES ON STAINLESS STEEL

W.F. Bailey, Jr.
S.S. Fisher

MEASUREMENT OF ADSORPTION STAY-TIMES OF SEVERAL ATMOSPHERIC GASES ON STAINLESS STEEL

by

W.F. Bailey, Jr.

and

S.S. Fisher

Technical Report

under

NASA Grant NGR-47-005-046

Department of Aerospace Engineering and Engineering Physics

RESEARCH LABORATORIES FOR THE ENGINEERING SCIENCES

SCHOOL OF ENGINEERING AND APPLIED SCIENCE

UNIVERSITY OF VIRGINIA

Charlottesville, Virginia

Report No. AEEP-4038-111-69U

June, 1969

FOREWORD

This report is the thesis of Mr. Bailey submitted in partial satisfaction of the requirements of the degree, Master of Aerospace Engineering, at the University of Virginia. The investigation described herein was carried out under the sponsorship of the National Aeronautics and Space Administration, through Grant NGR 47-005-046 and under the direction of the undersigned, a principal investigator with that grant. Other principal investigators with this grant are Professors A.R. Kuhlthau and J.E. Scott, Jr. Funds made available through the University of Virginia's NASA Institutional Grant NsG-682 were used for construction of much of the basic laboratory apparatus.

Sam S. Fisher
Assistant Professor
Aerospace Engineering

ABSTRACT

A preliminary experiment has been carried out using a simple time-of-flight method to determine mean times of adsorption of gaseous molecules on a solid surface. A room temperature aerodynamic molecular beam is pulsed by a slotted chopper disk, impinges on an "engineering surface," and a portion of the reemitted molecules pass through a density sensitive time-of-flight detector. The response (density versus time) of the detector is compared for two cases:

(1) diffuse emission of beam molecules from the test surface with zero stay time.

(2) diffuse emission of molecules from the test surface with a distribution of stay times.

The mean stay time is inferred from the shift in the maxima of the detector response for cases (1) and (2).

The "engineering surface" consists of a stainless steel target on which an undetermined combination of several more or less permanently adsorbed gases is present. Mean stay times of the order of 10^{-4} seconds have been observed for argon on this surface in the range of surface temperatures 80 to 100°K. Stay times of the order of 10^{-5} seconds have been observed for nitrogen and carbon dioxide in the ranges 92 to 97°K and 130 to 210°K respectively.

Due to the uncertain nature of the surface these preliminary results are not of quantitative value, but they do indicate that the time-of-flight method is feasible for the measurement of mean adsorption stay times.

ACKNOWLEDGMENTS

The author wishes to express his gratitude to Professor S. S. Fisher for patient advice and assistance throughout this research, and to Dr. M. N. Bishara whose practical advice on laboratory technique was invaluable. Thanks are also due to Mr. E. W. McClurken for help with the numerical analysis associated with this project and to Messrs. J. R. Bledsoe, and G. A. Pjura for aid rendered at various times during this work. While engaged in this research, the author was supported by an NDEA Title IV Fellowship.

TABLE OF CONTENTS

TABLE OF CONTENTS (continued)

TABLE OF CONTENTS (continued)

LIST OF FIGURES

LIST OF TABLES

LIST OF SYMBOLS

A_t	effective area of the beam footprint on the target
C	a constant, Eq. (3.3.1)
C_1	a constant, Eq. (3.3.4)
C_2	a constant, Eq. (3.3.5)
C_3	a constant, Eq. (3.3.6)
$\bar{E}_g$	average energy of molecules before striking a surface, Eq. (1.1.1)
$\bar{E}_r$	average energy of reemitted molecules, Eq. (1.1.1)
$\bar{E}_w$	average energy of thermally accommodated molecules, Eq. (1.1.1)
I	intensity (particles per unit area, per unit time)
k	Boltzmann's constant (1.38×10^{-16} erg/°K)
K_1, K_2	constants, Eq. (2.2.1)
ℓ_r	beam dimension in the direction radial to the chopper periphery, Fig. (3.2.2)
ℓ_t	beam dimension in the direction tangent to the chopper periphery, Fig. (3.2.2)
L	target-detector traverse length, Fig. (3.1.3)
m	molecular mass
n	number density
$n_d(t)$	detector density function, Eq. (3.3.1)
$N(t)$	number of particles adsorbed on surface at time t

LIST OF SYMBOLS (continued)

N_o	number of particles adsorbed at time zero, also equal to the total number of particles in a beam pulse
p	desorption probability per unit time
R	universal gas constant (= 1.987 $\frac{\text{calories}}{\text{mole-}^\circ\text{K}}$)
$\mathcal{R}$	time-of-flight resolution, Eq. (5.2.1)
$\mathcal{v}$	peripheral speed of chopper
s_r	chopper slot dimension in radial direction, Fig. (3.2.2)
s_t	chopper slot dimension in direction tangent to chopper periphery, Fig. (3.2.2)
$S(t)$	detector signal function, Eq. (3.3.2)
$S(t)_{\tau \neq 0}$	detector signal function modified by stay time distribution, Eq. (3.3.5)
t	time
t_m	time for which the detector response is a maximum
$t_m(\tau = 0)$	time for which the detector signal is a maximum if $\tau = 0$, Eq. 3.3.3)
$t_m(\tau)$	time for which the detector signal is a maximum if $\tau \neq 0$, Eq. (3.3.8)
$(t_m)_{\text{ROOM TEMP}}$	time for which the detector response is a maximum, with the target at room temperature, Eq. (4.2.1)
t_p	time duration of the beam pulse, Eq. (3.2.2)
δt	an increment of time
Δt	detector signal halfwidth
Δtp	beam pulse half-width, = $t_p/2$ if $\ell_t = s_t$

T	target surface temperature
U	heat of adsorption
U_o	(-) potential energy of an isolated adsorbed molecule
α	energy accommodation coefficient
β	$= (\frac{m}{2kT})^{1/2}$
β_R	value of β for T = room temperature
δ	time for the beam pulse to travel from the chopper slot to the target surface, Eq. (4.2.1)
σ	adsorption coverage (number of molecules adsorbed per unit area)
σ_o	adsorption coverage at time zero
τ	mean stay time of adsorbed molecules, Eq. (1.2.4)
τ_o	period of vibration of adsorbed molecules

Subscripts

m	denotes value of variable for which a function is a maximum
o	denotes initial value

Superscripts

—— (bar)	mean value
' (prime)	denotes variable of integration
$\sim$ (tilda)	denotes time variable made nondimensional by dividing by βL.

CHAPTER I

INTRODUCTION

1.1 Introductory

1.1.1 The Study of Gas-Surface Interactions

A fundamental problem in gasdynamics is the transfer of energy and momentum from a gas to a body moving through the gas. The practical result of solving this problem is the determination of heat transfer to the body and the aerodynamic forces on the body. In the continuum region of flow the problem is approached on a macroscopic level, and only bulk properties of the gas need to be studied. In the low density regime of flow however, the problem must be approached from a molecular point of view. The details of the interaction between the molecules of the gas and the solid surface are important.

A great deal of work in the study of gas-surface interactions has involved the experimental measurement of accommodation coefficients. An accommodation coefficient is a parameter expressing the degree to which the molecules of a gas reach equilibrium with some property of a solid surface. For example, the coefficient of thermal accommodation, α, is usually defined[1] as:

$$\alpha = \frac{\bar{E}_g - \bar{E}_r}{\bar{E}_g - \bar{E}_w} \qquad (1.1.1)$$

$\bar{E}_g$ is the average energy of gaseous molecules before striking the surface, $\bar{E}_r$ is the average energy of the molecules after reemission from the surface, and $\bar{E}_w$ is the average energy the reemitted molecules would have if they were to come to thermal equilibrium with the surface. The accommodation coefficient is an average over a large number of molecules, and leaves undetermined the detailed mechanism of the gas-surface interaction. Furthermore, α is a function of several variables such as the temperature of the surface, the temperature of the gas, and the nature of the adsorbed gaseous layer[2]. Therefore, knowledge of the mechanism of interaction would be useful in the determination of the relative importance of the several variables influencing the accommodation coefficients as well. Of course, this is just one example of many areas of gas-surface research which would benefit from a detailed understanding of the interaction mechanism.

1.1.2 Adsorption

Langmuir[3] in 1916 proposed that, for a great many situations in which gaseous molecules strike a solid

surface, true reflection of the molecules (specular or diffuse) does not occur to an appreciable extent, but rather the molecules spend a finite time on the surface even though this time might be so small that the molecules appear to rebound instantaneously from the surface by macroscopic standards. The phenomenon in which a gaseous molecule strikes a solid surface and is held on the surface for a finite time is known as adsorption. The time during which the molecule remains on the surface is referred to as the stay time or residence time. If the forces effecting the adsorption are of the Van der Waal's type, the process is known as physical adsorption. If the forces are of a chemical binding nature, the process is known as chemical adsorption. We will henceforth be concerned with one aspect of physical adsorption, namely, the measurement of the mean stay time of a large number of physisorbed molecules.

1.2 Background

1.2.1 Significance of the Mean Stay Time

The physical significance of the mean stay time is made clear by the case in which a molecular beam (directed stream of gas molecules) of constant intensity, I, strikes a solid surface and is adsorbed thereon. If equilibrium

is established, then the number of molecules arriving at the surface per unit area per unit time must be equaled by the number leaving per unit area per unit time:

$$I = \sigma \cdot p \qquad (1.2.1)$$

where σ is the number of molecules adsorbed per unit area, and p is the probability of desorption per unit time. Let the molecular beam be terminated at time t = 0. At the instant the beam stops, there is a number, N_o, of molecules adsorbed on the surface. As desorption proceeds, the number, N(t), of molecules still remaining on the surface decreases. The number, dN, leaving the surface in an increment of time dt at time t is then

$$dN = N(t)\, p\, dt \qquad (1.2.2)$$

Assuming that p is not a function of coverage, it follows that N(t) can be written[4] as:

$$N(t) = N_o \exp(-pt) \qquad (1.2.3)$$

Let us now define the mean stay time of this group of N_o molecules as[5]:

$$\tau \equiv \frac{1}{N_o} \int_o^\infty t \left(\frac{dN}{dt}\right) dt \qquad (1.2.4)$$

$\frac{dN}{dt}$ can be obtained from Equation (1.2.3) and substituted in (1.2.4). Then (1.2.4) can be integrated by parts to give:

$$\tau = \frac{1}{P} \qquad (1.2.5)$$

The physical significance of the mean stay time is that it is the reciprocal of the desorption probability per unit time [4,5,6].

1.2.2 Frenkel's Equation for the Mean Stay Time

Frenkel[4], using the theory of statistical mechanics, obtained an expression relating the mean stay time to the temperature, T, of the adsorbing surface and the potential energy, U_o, of an isolated molecule adsorbed on the surface:

$$\tau = \tau_o \exp\left[\frac{U_o}{RT}\right] \qquad (1.2.6)$$

τ_o is the period of oscillation of adsorbed molecules and has the same order of magnitude as the period of vibration of the atoms of the solid surface. Therefore, the order of magnitude of τ_o is between 10^{-12} and 10^{-14} seconds[6].

Equation (1.2.6) is derived on the assumption that the number of adsorbed molecules per unit area of surface is sufficiently small to ignore interactions between adsorbed particles in the determination of the heat of adsorption (energy necessary to remove a molecule from the adsorbed state) and the determination of the period of vibration of the adsorbed molecules. Equation (1.2.6) can be extended to situations in which the value of σ is not small enough to neglect interactions between adsorbed molecules. If the heat of adsorption is given by:

$$U = U_o + i\Delta U \qquad (1.2.7)$$

where ΔU is the additional potential energy associated with a bond between adsorbed molecules, and i is the number of such bonds, then the stay time for a given particle bonded to i neighbors obeys[4]:

$$\tau^{(i)} = \tau_o \exp\left[\frac{U_o + i\Delta U}{RT}\right] \qquad (1.2.8)$$

If the value of i is the same for all adsorbed molecules, then

$$\tau = \tau_0 \exp\left[\frac{U_0 + i\Delta U}{RT}\right] = \tau_0 \exp\left[\frac{U}{RT}\right] \quad (1.2.9)$$

For any case in which the adsorbed molecules have much less affinity for each other than for the solid surface, the process will be limited to the formation of a monomolecular layer. That is, molecules striking the adsorbed layer will see a relatively weak attraction as compared to the attraction between the surface and the molecules of the monolayer. It follows from Equation (1.2.6) that the mean stay times of molecules in layers past the first are negligible. This is the case for a gas adsorbing on the surface of a metal[4].

1.2.3 Previous Stay-Time Measurements and Objects of Experiment

Stay-times have been measured by experimenters previous to this investigation. Particularly noteworthy are the results of Clausing[7] who used observations of flow-through times of several gases through glass capillaries to infer mean stay times on the capillary walls. More recently, Leonas[8] reported measurements of stay times of

argon and carbon dioxide on technical grade surfaces of Cu, Fe, and Ta, using a molecular beam time-of-flight technique. However, the total information available on stay times is very small, and a great deal of experimentation remains to be carried out. Therefore this research was undertaken with the following objectives:

(i) Set up a preliminary experiment to test the feasibility of a time-of-flight method for the measurement of mean stay times using the aerodynamic molecular beam facility available at the University of Virginia.

(ii) Obtain measurements of adsorption stay-times for several readily available laboratory gases on an engineering surface.

CHAPTER II

ANALYSIS

2.1 Factors Influencing the Mean Stay Time

In theory, the heat of adsorption U, is not directly dependent upon the surface temperature. However, in general, U is a function of the coverage, σ , of the adsorbate under consideration as well as the amount of coverage of other gases adsorbed on the surface. The dependence of U on σ is due to two effects. First, if the surface is considered to have a definite number of adsorption sites, adsorption will take place first at those sites for which the heat of adsorption has the greatest values[6]. Thus, as σ increases from zero, the average value of U will decrease. Second, as σ increases, interactions between adsorbed molecules begin to make a contribution to the heat of adsorption. The same effects may be observed in the case of increasing coverage of any additional gas adsorbed on the surface. Therefore, in any experiment the heat of adsorption will be a function of the coverage of the adsorbate under consideration as well as the coverage of other adsorbates (where other adsorbates refers to the unavoidable background gases present in any experimental apparatus). Since the coverage may be a function of both surface temperature and time, the heat of adsorption may be a function of temperature and time.

The vibrational period τ_o depends only on the gas-surface combination[6]. But again, since the nature of the surface is dependent upon the coverage of adsorbed gases, one might expect values of τ_o deduced from experimentation to be dependent on temperature and time also.

In view of the above considerations, Equation (1.2.9) can be written:

$$\tau = \tau_o(T,t) \exp\left[\frac{U(T,t)}{RT}\right] \qquad (2.1.1)$$

If surface coverage has reached equilibrium (is not time dependent), then:

$$\tau = f(T) \qquad (2.1.2)$$

where f denotes an unknown functional relationship between the mean stay time and the temperature of the surface.

2.2 Ideal Experimental Conditions for Stay-Time Measurement

Ideally, we would like to produce experimental conditions for which U and τ_o are constant. Then Equation (1.2.9) could be used to specify the exact dependence of the mean stay time on temperature. By varying the surface temperature for a given gas-surface combination, the

dependence of τ on T could be determined experimentally and compared to the theory as given by an equation of the form:

$$\tau = K_1 \exp\left(\frac{K_2}{T}\right) \qquad (2.2.1)$$

K_1 and K_2 are constants for a particular experiment. For situations in which Equation (2.2.1) applies, it is readily apparent that the mean stay times to be measured can be made as large as experimental resolution limitations require simply by lowering the surface temperature sufficiently.

In order to achieve constant U and τ_o experimentally, the following requirements must be satisfied:

1. σ must be so small that adsorbed molecules are effectively isolated from one another.
2. The heat of adsorption and period of vibration must be the same for all adsorption sites.
3. The coverage of other gases on the surface must be entirely negligible.

While one might expect to produce adsorption at low coverage, it is unrealistic to expect to find any real surface which would satisfy the second restriction. Probably the best that can be done in practice is to satisfy the first and third requirements, and then, after making experimental measurements of τ, try to deduce

from the experiments whether U and τ_0 are strongly dependent upon adsorption site. For example, after providing for low coverage, the experiments could be conducted and the time-equilibrated measurements of τ then interpreted in the following form:

$$\tau = \tau_0(T) \exp\left[\frac{U(T)}{RT}\right] \qquad (2.2.2)$$

To the extent that $U(T)$ and $\tau_0(T)$ are constant over the experimental range of temperatures, it could be concluded that they are site independent. In the next section, guided by these considerations, an experiment is proposed for the measurement of mean stay times.

2.3 Ideal Experimental Method

Consider a molecular beam of constant intensity striking a metallic surface. It is desired to interrupt the beam periodically causing pulses of sufficiently short duration to insure that:

1. All particles in a pulse strike the target within an interval of time, δt, which is much smaller than the mean time of adsorption.
2. The maximum coverage of particles adsorbed in the area of intersection of the beam and the target is small enough to neglect

consideration of the interactions
between adsorbed particles.

On the other hand, the time between successive pulses should be sufficiently large so that all but a negligible fraction of the molecules in one pulse will be desorbed from the surface before the next pulse begins. If a detection device sensitive to the number density of particles passing through it at a given time is placed in a position to intercept a portion of the desorbing particles, a record of the desorption process as a function of time can be obtained, and the mean stay time may be inferred from this record.

It should be noted that, since the number of particles in each pulse is constant and the area of the beam at the target is constant, the coverage σ is the same for all target temperatures. However, σ is not uniform over the target surface as a result of the variation of intensity over the beam cross-section. The maximum value, σ_{max}, of the coverage over the beam footprint is much less than that required for a monolayer of adsorbed particles. Therefore, the heat of adsorption of the beam gas is only dependent upon the other gases adsorbed on the target. These other gases:

1. would be no problem if their coverage were so small as to have no effect.

or;

2. would, if their coverage time-equilibrated rapidly enough, only introduce an uncertainty in the makeup of the test surface.

A practical method of controlling the coverage of other gases on the surface consists of continuously depositing a known gas on the surface at a rate sufficient to guarantee its preponderance over other adsorbed gases. If this process is carried to the point at which the known gas effectively becomes the adsorbing surface, the coverage will certainly be a constant, and Equation 2.2.1 will apply. This method would also eliminate the uncertainty in the makeup of the test surface.

2.4 Model of the Adsorption - Desorption Process

Assuming that the molecules adsorbed on the target surface have a mean stay time several orders of magnitude greater than the characteristic time of surface vibration, it is entirely reasonable to expect that the adsorbed molecules undergo complete thermal accommodation with the surface[3]. In addition, thermal accommodation has been verified independently at the temperatures of interest in this investigation in a separate experiment conducted by the author. Therefore, the molecules depart the surface diffusely with a Maxwellian distribution of speeds

corresponding to the surface temperature. Now consider the following model. At time zero, corresponding to the mean arrival-time of the pulse at the target, there are N_o particles adsorbed on the surface. Let us assume that the desorption probability p is independent of coverage. Under these conditions Equation (1.2.3) applies, and since $\tau = \frac{1}{p}$, we have for the number, N, of molecules remaining on the surface as a function of time:

$$N(t) = N_o \exp\left(-\frac{t}{\tau}\right) \qquad (2.4.1)$$

2.5 Choice of Test Gas and Surface Conditions

Argon, carbon dioxide, and nitrogen were readily available in the laboratory and were considered as possible test gases. The time-of-flight method of measuring stay times, as set up in this investigation, had a time resolution of about 10^{-5} seconds (see Chapter V). Therefore, it was necessary to choose gases and surface conditions for which stay times of the order of 10^{-4} seconds or more could be observed.

No method of protecting the target surface from background gas adsorption was considered initially. For the purpose of this preliminary experiment, a stainless steel target of machine smoothness was adopted. Of course,

the surface of the stainless steel was not at all that of the bulk; it undoubtedly consisted of an oxide layer and possibly a number of more or less permanently adsorbed constituents. For the purpose of a feasibility experiment such as this, however, the exact nature of the surface is of little consequence.

Using estimated values of U based on the average heat of adsorption of Ar, CO_2, and N_2 on a variety of surfaces and a value of τ_o calculated from an expression giving the period of vibration of surface atoms of stainless steel[6], expected stay times were calculated at various surface temperatures. These calculations are tabulated in Table 2.5.1.

As expected, and as apparent from Table 2.5.1, cooling of the target surface is necessary to bring about measurable stay times. Furthermore, for argon and nitrogen, temperatures of 100°Kelvin or lower (such as are attainable with liquid nitrogen cooling) must be reached. As will be seen later, the expected effect of surface contamination due to other adsorbates is to decrease the stay times from the values indicated above, so that cooling the target to temperatures below even that of liquid nitrogen might be desirable.

TABLE 2.5.1

MEAN STAY TIMES OF SEVERAL GASES ON STAINLESS STEEL AS A FUNCTION OF SURFACE TEMPERATURE

GAS	TEMP $_{(°K)}$	τ_o (sec)	U ($\frac{kcal}{mole}$)	τ (sec)
ARGON	80	2.0×10^{-13}	4.0	1.4×10^{-2}
	90			1.2×10^{-3}
	100			9.7×10^{-5}
NITROGEN	80			1.4×10^{-2}
	90			1.2×10^{-3}
	100			9.7×10^{-5}
CARBON DIOXIDE	150		8.0	8.1×10^{-2}
	200			9.7×10^{-5}
	300			1.2×10^{-7}

CHAPTER III

EXPERIMENTAL APPARATUS

3.1 Introductory

3.1.1 Time-of-Flight Method

An aerodynamic molecular beam,[9,10] after suitable collimation, strikes a rapidly rotating disk with slots located on its periphery which allow short pulses of the beam to strike the target (Figure 3.1.1). The disk has four diametrically opposed slots. When the beam is centered in a slot, a high intensity light beam is centered in the opposite slot, giving an electrical impulse to a photosensitive field-effect transistor. The generated photopulse fixes the start of each molecular pulse, and the inverse frequency of photopulses gives the time between molecular pulses.

The molecules strike the target, adsorb on the surface, and are reemitted diffusely (diffuse reemission has also been established independently by the author). A portion of the molecules strike the detector, which in turn ionizes a small fraction (about 0.1%) of them and collects the positive ions. The response of the detector is therefore a positive ion current. Since the molecules in any pulse have a distribution of speeds and stay times,

they reach the detector at different times, and the ion current varies with time.

After suitable amplification, much of the noise is averaged out of the detector signal with a waveform eductor (Princeton Applied Research, Model TDH-9), and the signal is plotted on a chart recorder. The waveform eductor, triggered by the photopulse, operates by averaging over a large number of repetitive pulses. The photopulse signal is superimposed on the averaged detector response, and the combined signal is fed to the chart recorder. Figure 3.1.2 shows two typical recordings of the photopulse and detector response signals.

3.1.2 The Vacuum System

The experiment is carried out in a large vacuum chamber (Figure 3.1.3). This chamber, primarily of stainless steel construction, is partitioned into three smaller chambers. The molecular beam is formed in a first chamber, collimated in a second, and passes into a third chamber where the chopper, target, and detector are located. The pressure in the first chamber is about 10^{-3} torr, in the second chamber is about 10^{-5} torr and in the third or test chamber is of the order of 10^{-7} torr.

The test chamber is equipped with a liquid nitrogen cold trap located above the oil diffusion pump (using

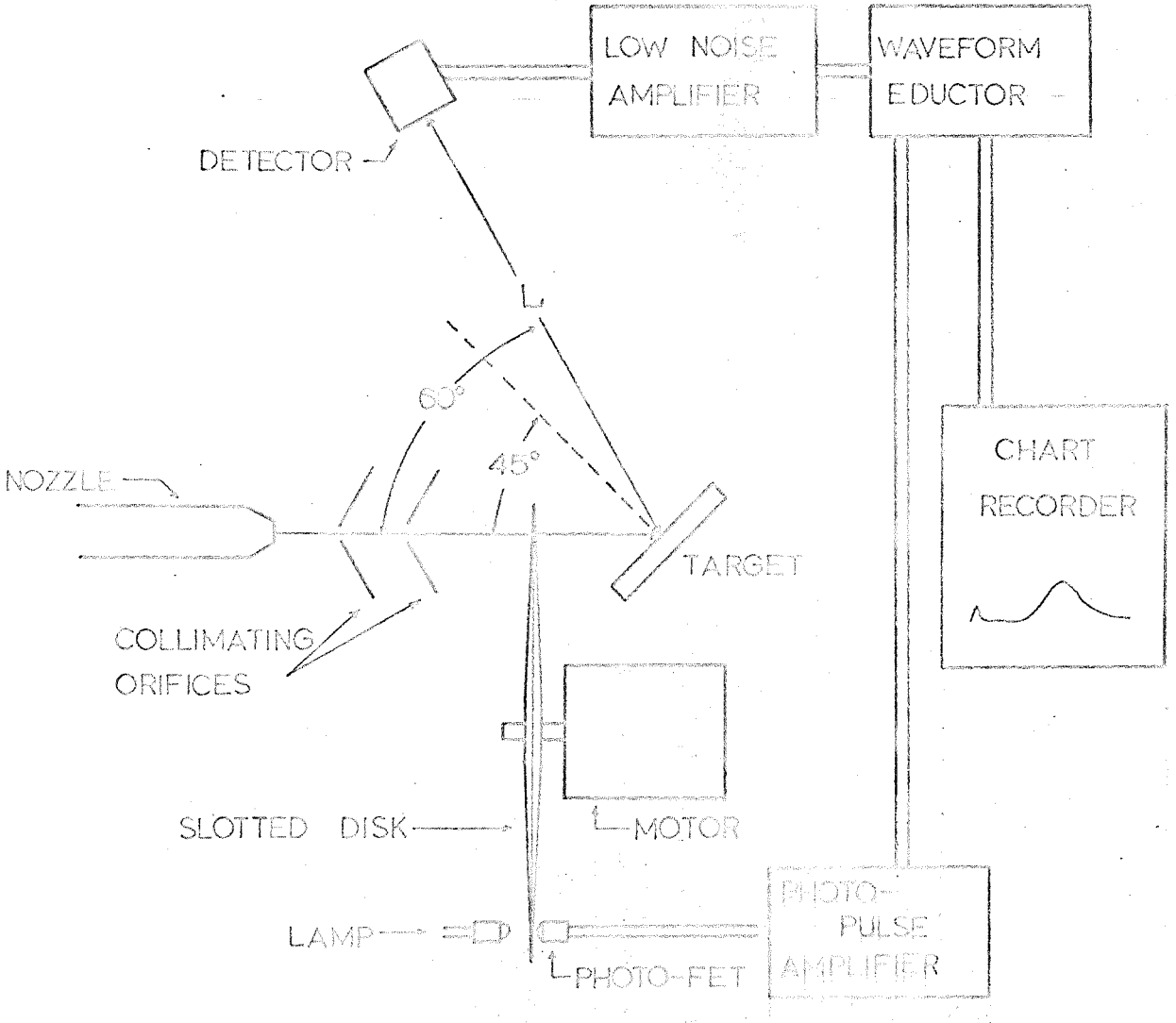

FIGURE 3.1.1 SCHEMATIC DIAGRAM OF THE TIME-OF-FLIGHT METHOD

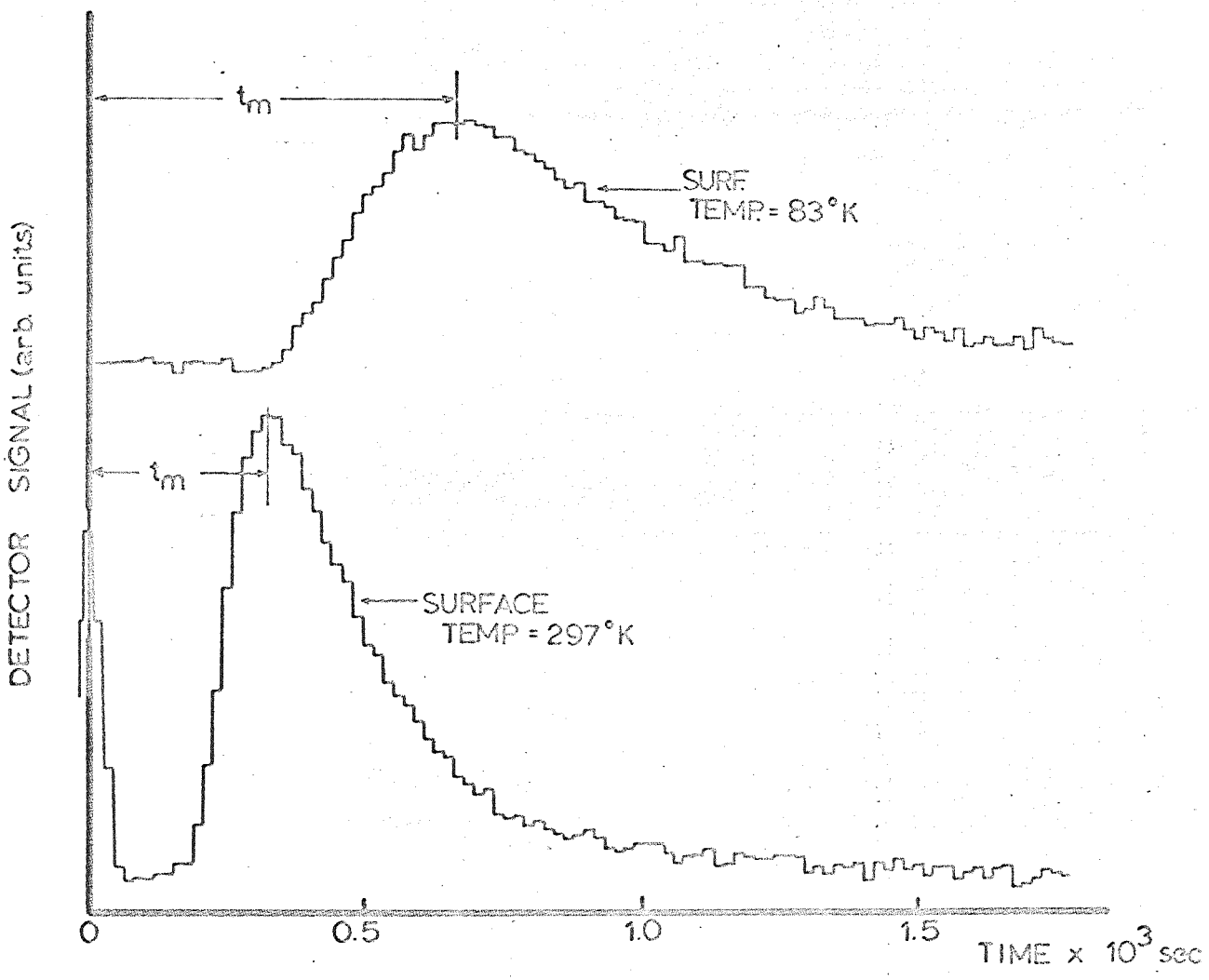

FIGURE 3.1.2 TYPICAL CHART RECORDINGS OF THE DETECTOR SIGNAL

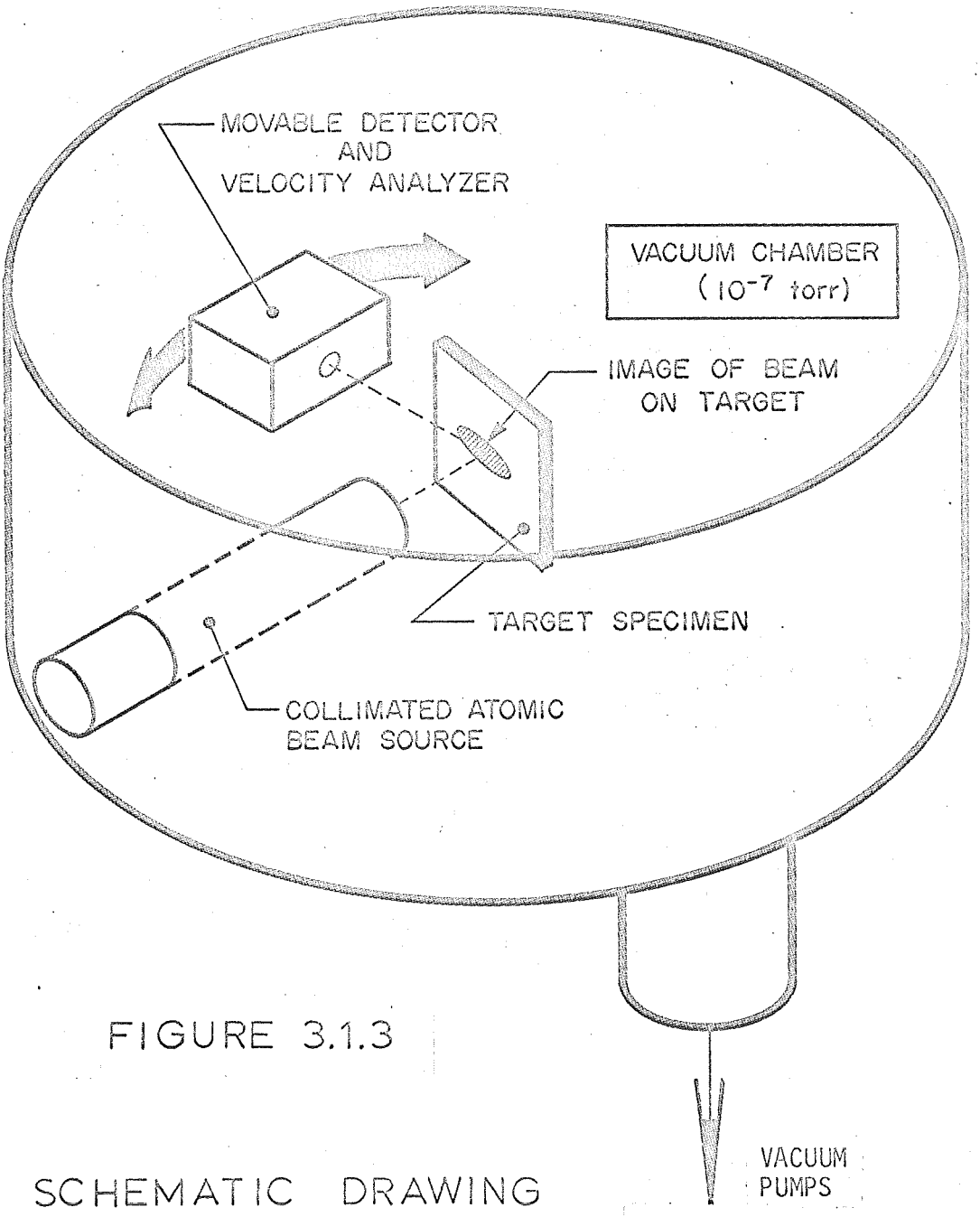

FIGURE 3.1.3

SCHEMATIC DRAWING

OF THE EXPERIMENTAL APPARATUS

DC-705 fluid) and a minimum test chamber background pressure of 2×10^{-7} torr was achieved. During the course of the experiment, pressures in this chamber varied between 2×10^{-7} and 8×10^{-7} torr. Mass spectrometer analysis of the background gases in this chamber showed the principal constituents to be 18 amu (H_2O) and 28 amu (CO or N_2).

The most complete discussion of the details of the molecular beam and detector characteristics as well as the construction of the vacuum system can be found in the report of Hagena et al[11].

3.2 Design Considerations

3.2.1 The Target Holder

The target is a block of type 304 stainless steel having a one-inch-square face welded to a cylindrical stainless steel tank (Figure 3.2.1). The top of the tank is welded to a flange having an O-ring seal. The entire holder assembly is inserted into the test chamber through a hole in the top wall of the vacuum chamber. The division of the reservoir into two cylinders of different diameter maximizes the capacity of the reservoir while allowing it to clear obstacles in the test chamber. The reservoir is filled with liquid nitrogen by means of a filler pipe extending through the flange.

FIGURE 3.2.1

THE TARGET HOLDER

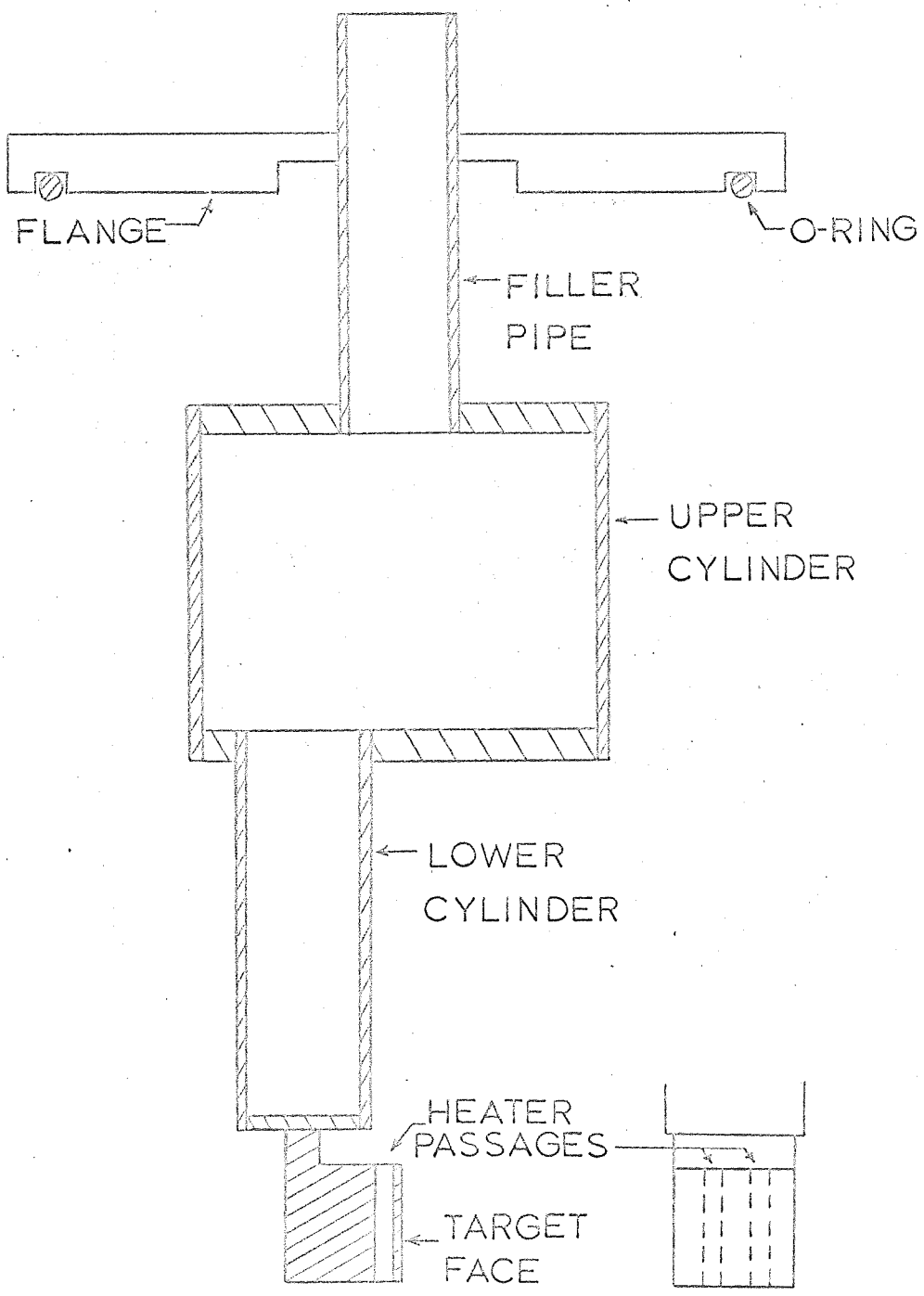

The temperature of the target surface can be controlled by means of a pair of tungsten heater coils passing just under the target surface. Foil radiation shields spot-welded to the target block prevent unnecessary boiloff of liquid nitrogen due to radiation from the heater coils. The coils are encased in quartz tubes which provide the necessary electrical insulation while allowing radiative heat transfer to the target block.

Measurement of the surface temperature is accomplished by means of a chromel-alumel thermocouple junction spot-welded near the target face.

3.2.2 Beam Modulation

The beam modulation system consists of the collimating orifices, the chopper, and the detector. There are two primary considerations in the design of the beam modulation system.

1. Resolution of time.
2. Sufficient intensity of particles arriving at the detector to provide reasonable signal-to-noise ratio.

For optimal time resolution, it is necessary to make the duration of the beam pulse as short as possible. To state this condition more precisely, let the molecular beam have a cross-sectional area at the chopper disk

characterized by a length ℓ_t in the direction tangent to the chopper periphery and ℓ_r in the radial direction (Figure 3.2.2). Let the width of the chopper slot in the tangential direction be s_t and in the radial direction s_r. If the peripheral speed of the disk is ρ, then it is required that

$$t_p \equiv \text{pulse width} \equiv \frac{s_t + \ell_t}{\rho} << \tau \qquad (3.2.2)$$

Obviously, t_p can be made as small as desired simply by increasing the speed ρ. However, as t_p is decreased in this way, the total number of particles reaching the target in a given pulse decreases, with a consequent loss of intensity at the detector.

Aside from intensity considerations, there are practical limitations on the chopper speed. A definite speed limitation exists due to structural considerations of the bursting strength of the disk. Also, there is some finite capability of the motor used to drive the disk. Another important limitation is that the period between successive pulses should be large compared to the time half-width, Δt, of the detector response in order to avoid overlap. These are general limitations which might be encountered in any particular experiment. Fortunately, however, in this experiment, these practical limitations were not approached. Instead, the intensity consideration proved to be crucial.

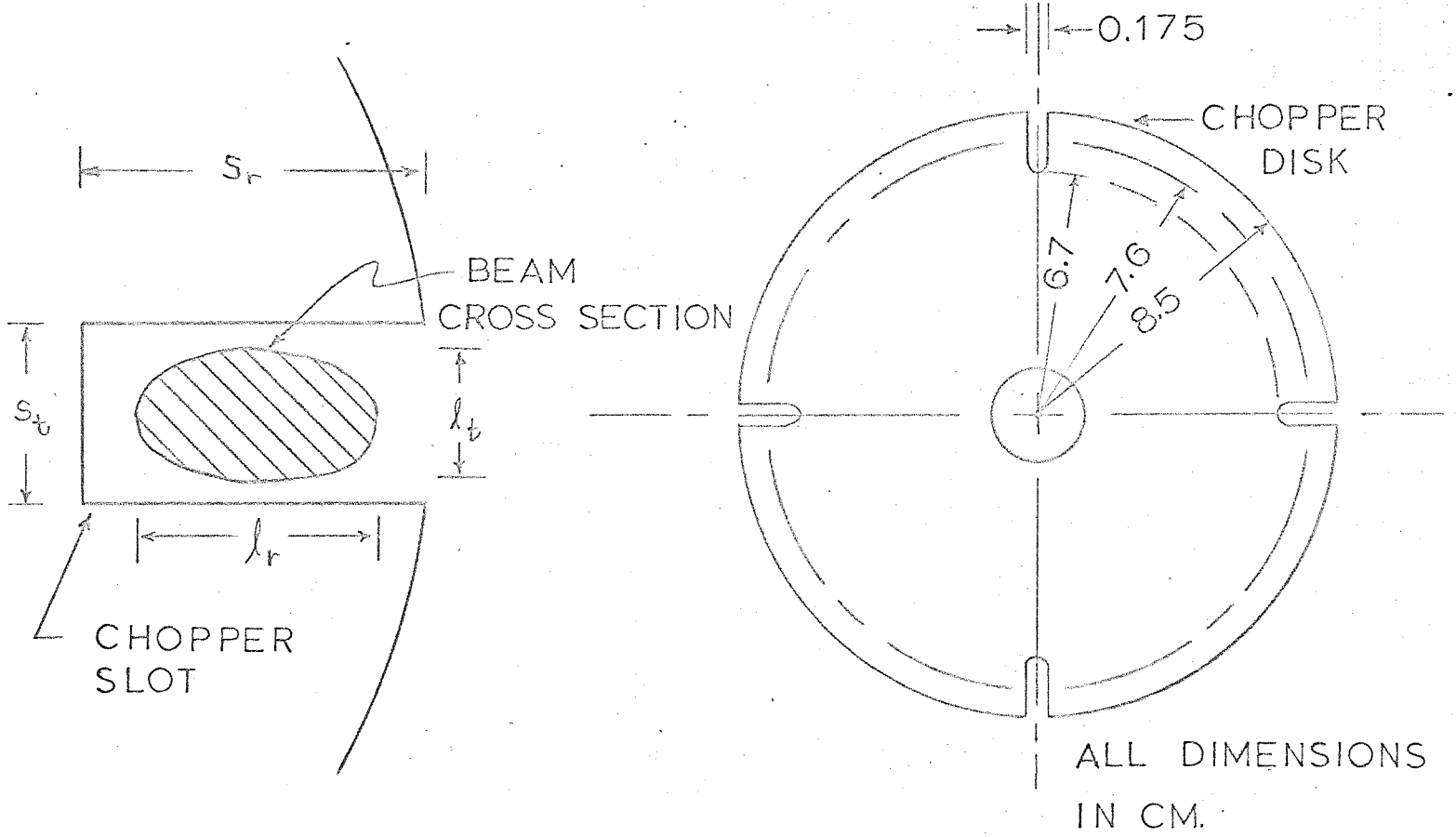

FIGURE 3.2.2 CHOPPER GEOMETRY

For maximum intensity at the detector, and thus, maximum signal to noise ratio, the detector should be placed a distance as short as possible from the target surface. In this vacuum system, the geometry of the test chamber prevented the detector from being placed any closer than 11.5 cm. from the target and this is where it was placed. This being done, the chopper was operated at the highest speed for which reasonably strong detector signals could be obtained.

There are several secondary considerations in the design of the beam modulation system. The first of these is the placement of the detector relative to the target normal direction. For diffuse emission of the desorbing particles, the intensity seen by the detector will be a maximum in the direction normal to the target surface, and thus optimal placement is along this normal. The second consideration is the angle between the target normal and the beam direction. Ideally, this angle should be minimized to minimize in turn the area of the target intersected by the incident beam, thus providing better angular resolution for the detector. A best selection (consistent with geometrical constraints) of 45° for the angle of incidence, and 15° for the angle of reflection was made.

The measurement of stay times required that the chopper be moved from its usual location in other experiments performed in this laboratory (between the target and the

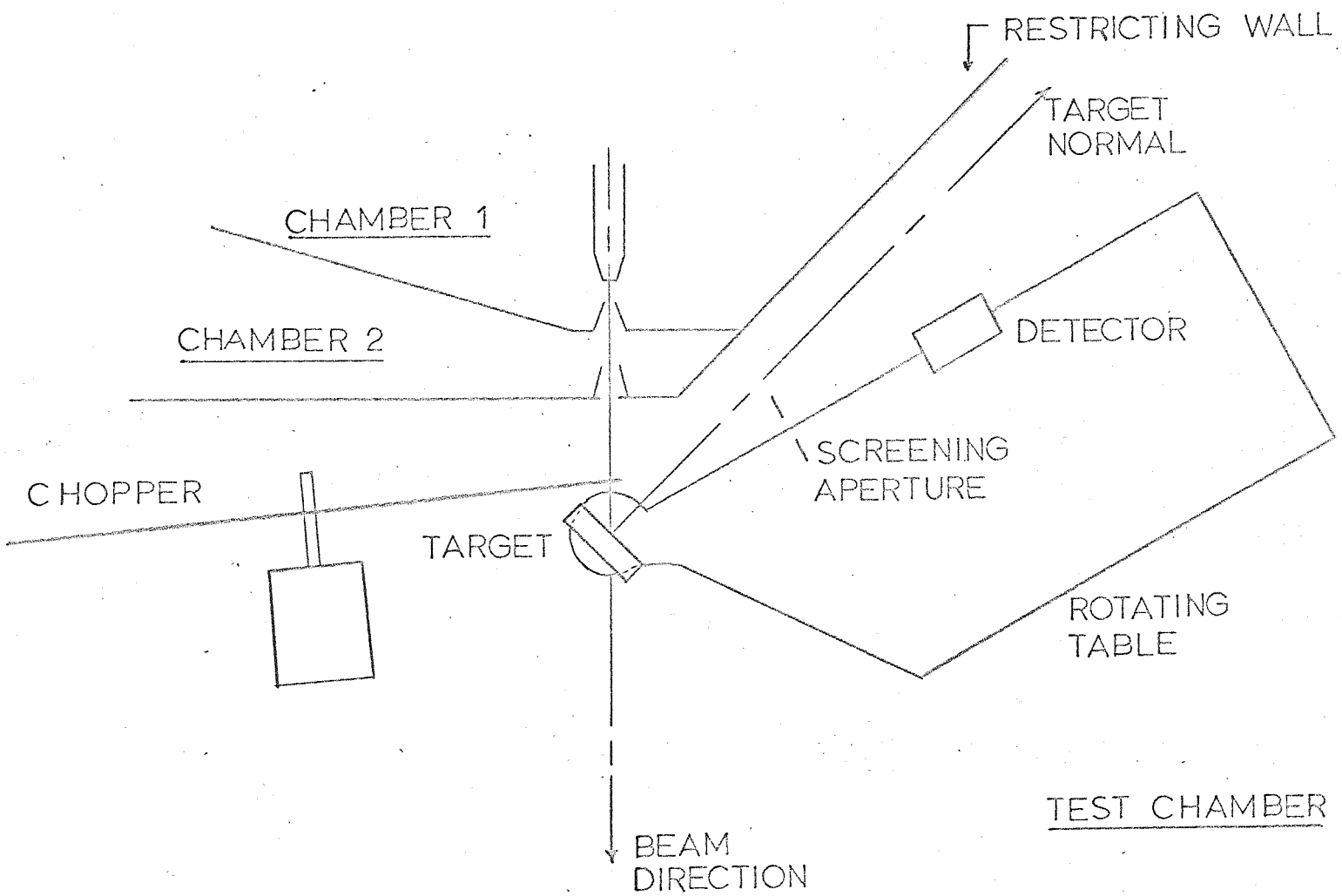

FIGURE 3.2.3 GEOMETRY OF THE TEST CHAMBER

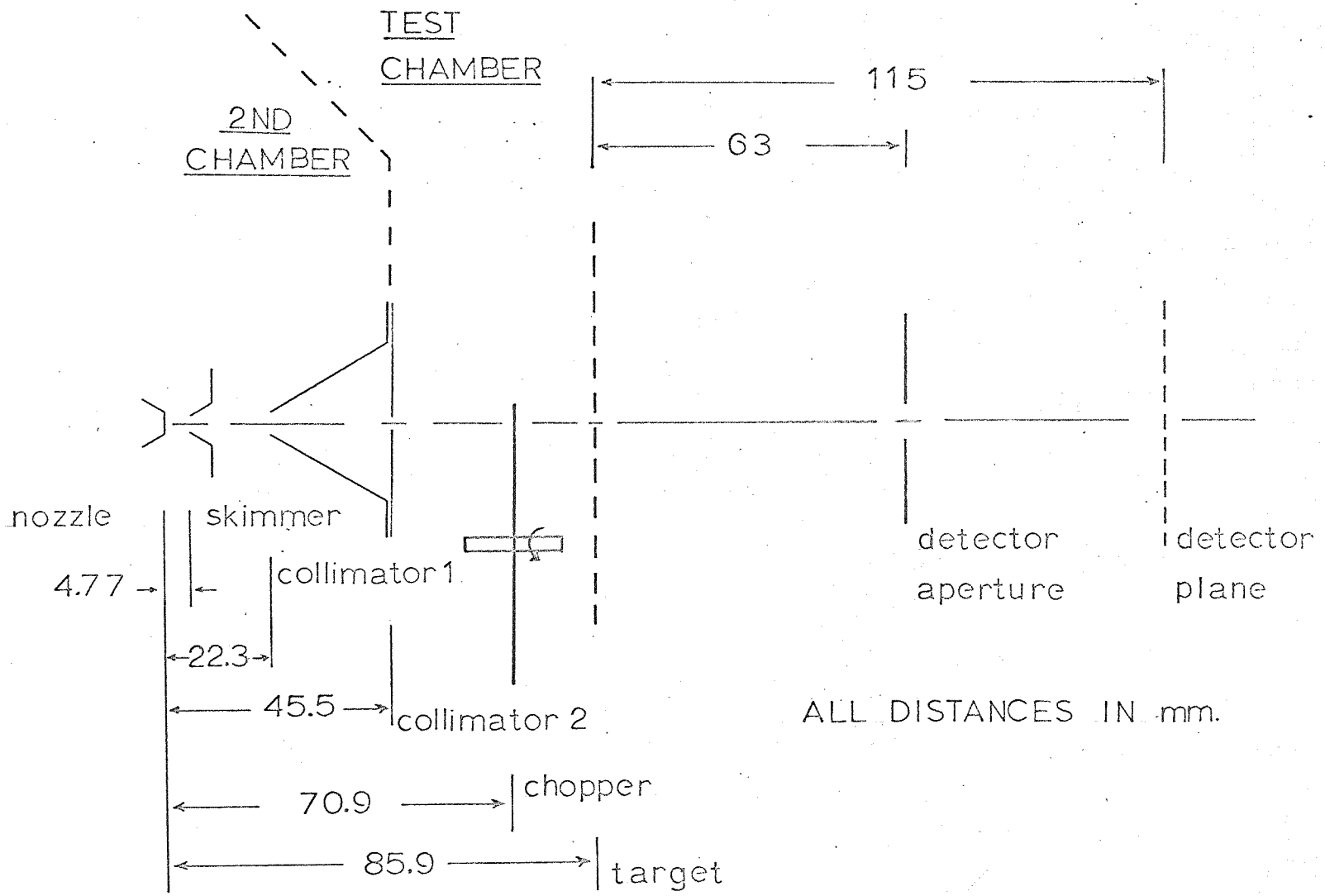

FIGURE 3.2.4 GEOMETRY OF THE BEAM MODULATION SYSTEM

detector) to a location between the collimator and the target (Figure 3.2.3). As in the case of the detector, geometric constraints determined the exact position of the chopper. Hagena et al have suggested that $\ell_t = s_t$ is an effective compromise between intensity and resolution[10]. Since, the collimating arrangement already in use in the vacuum system was not adequate to satisfy this constraint for the new location of the chopper, a third orifice was added which diminished the beam dimension, ℓ_t, at the chopper to the width s_t (= 1.75 mm) of the chopper slot.

Finally, desorbing particles striking areas adjacent to the detector active zone and eventually scattering into the detector may give rise to a spurious signal. To prevent this, a final aperture was placed between the target and the detector. Figure 3.2.4 gives a schematic representation of the entire beam modulation system.

3.3 The Form of the Detector Response

3.3.1 Response for the Limit as τ Approaches Zero

The ideal model of the adsorption-desorption process in this experiment has been discussed in Section 2.4. We now wish to consider the response of the detector as a function of time for this ideal model. The assumption of unit thermal accommodation of the adsorbed molecules to the surface temperature is fundamental in this analysis, and

is confirmed a posteriori by the magnitude of the stay times measured in the experiments.

Consider the response of the detector to a single pulse of molecules adsorbed on the target surface. Initially, these molecules have an average coverage density $\overline{\sigma}_o$. This two-dimensional layer of adsorbed molecules can be thought of as a three-dimensional gas in a box, and the target surface can be replaced by a shutter in one wall of the box. The molecules of the gas have a number density n_o proportional to $\overline{\sigma}_o$, and have a Maxwellian distribution of velocities corresponding to the temperature of the surface. Let the molecules reemitted from the target surface be thought of as streaming through this shutter of area A_t (equal to the effective area of the beam footprint on the target) into a region of sufficiently low pressure that the flow is free molecular. Now consider the number density $n_d(t)$ of molecules arriving at a detector a distance L from the shutter when the shutter is opened for an infinitesimal interval $\delta t'$ at $t = t'$. It is straightforward to show that this density obeys the following relation (see Appendix I).

$$n_d(t) = n_o \, \delta t' \, C \, (t-t')^{-4} \exp\left[\frac{-\beta^2 L^2}{(t-t')^2}\right] \qquad (3.3.1)$$

$$\beta = \left(\frac{m}{2kT}\right)^{1/2}$$

where C is a constant independent of time. Now the detector signal S(t) is proportional to the density $n_d(t)$ so that:

$$S(t) = n_o \delta t' C_1 (t-t')^{-4} \exp\left[\frac{-\beta^2 L^2}{(t-t')^2}\right] \qquad (3.3.2)$$

where C_1 is equal to C multiplied by a constant of proportionality. The value of time, t_m, corresponding to a maximum of S(t) for zero stay time is easily shown to be:

$$t_m(\tau=0) = t' + \beta L/\sqrt{2} \qquad (3.3.3)$$

3.3.2 Response as Modified by a Distribution of Stay Times

Now let us consider the case in which the molecules all strike the target at time t = 0, but have an exponential distribution of stay times with mean value τ such that the effective number density of molecules remaining adsorbed on the surface at any time t is $n_o \exp(-t/\tau)$. The detector signal in this case can be thought of as the integral of dS (t,t') over t' where $0 \leq t' \leq t$, and

$$dS(t,t') = n(t') C_1 (t-t')^{-4} \exp\left[\frac{-\beta^2 L^2}{(t-t')^2}\right] dt' \qquad (3.3.4)$$

$$n(t') = n_o \exp\left(-\frac{t'}{\tau}\right) \; ; \; \tau \neq 0$$

Formally integrating over t';

$$S(t)_{\tau\neq 0} = \int_0^t dS(t,t') = C_2 \int_0^t (t-t')^{-4} \exp\left[-\frac{t'}{\tau} - \frac{\beta^2 L^2}{(t-t')^2}\right] dt' \qquad (3.3.5)$$

where $C_2 = n_o C_1$. Introducing dimensionless times:

$$\tilde{t} = \frac{t}{\beta L} \quad , \quad \tilde{t}' = \frac{t'}{\beta L} \quad , \quad \tilde{\tau} = \frac{\tau}{\beta L}$$

the detector response is then

$$S(\tilde{t})_{\tilde{\tau}\neq 0} = C_3 \int_0^{\tilde{t}} (\tilde{t}-\tilde{t}')^{-4} \exp\left[-\frac{\tilde{t}'}{\tilde{\tau}} - (\tilde{t}-\tilde{t}')^{-2}\right] d\tilde{t}' \qquad (3.3.6)$$

where $C_3 = C_2/\beta^3 L^3$.

Now if τ is much less than $t_m(\tau = 0) = \beta L/\sqrt{2}$ (or, in other words, if $\tilde{\tau} << 1$) it can be shown (Appendix II) that the value of dimensionless time corresponding to a maximum of $S(\tilde{t})$ is given by:

$$\tilde{t}_m(\tilde{\tau}) \doteq 1/\sqrt{2} + \tilde{\tau} \qquad (3.3.7)$$

Reintroducing dimensional quantities and solving for τ:

$$\tau \doteq t_m(\tau) - \beta L/\sqrt{2} \qquad (3.3.8)$$

This result in Equation (3.3.8), says that for mean stay times which are small compared to the value of time for the response maximum, the stay time is given simply by the shift in the maxima of the response curves for the cases $\tau \neq 0$ and $\tau = 0$. Of course, the response of the detector for the case $\tau = 0$ is not determined experimentally, but is calculated from Equation (3.3.3) (this has been verified independently[9]).

The exact value of $\tilde{t}_m(\tilde{\tau})$ can be obtained from Equation(3.3.6) by using numerical methods to find the value of $\tilde{t}$ for which the integral

$$\int_0^{\tilde{t}} (\tilde{t}-\tilde{t}')^{-4} \exp\left[-\frac{\tilde{t}'}{\tilde{\tau}} - (\tilde{t}-\tilde{t}')^{-2}\right] d\tilde{t}'$$

is a maximum. The results of this analysis are shown in Figure 3.3.1, which is a plot of $\tilde{t}_m(\tilde{\tau})$ as a function of $\tilde{\tau}$. Note that for small values of $\tilde{\tau}$, $\tilde{t}_m(\tilde{\tau})$ approaches the value given by the approximation given by Equation(3.3.7). In the range of experimental data ($\tilde{\tau}<0.3$) the error in the determination of τ using the approximate relation, Equation(3.3.7), is no greater than 10 per cent. The details of the numerical analysis are discussed in Appendix III.

It should be noted that in the preceding discussion it is assumed that all the particles in a given pulse arrive

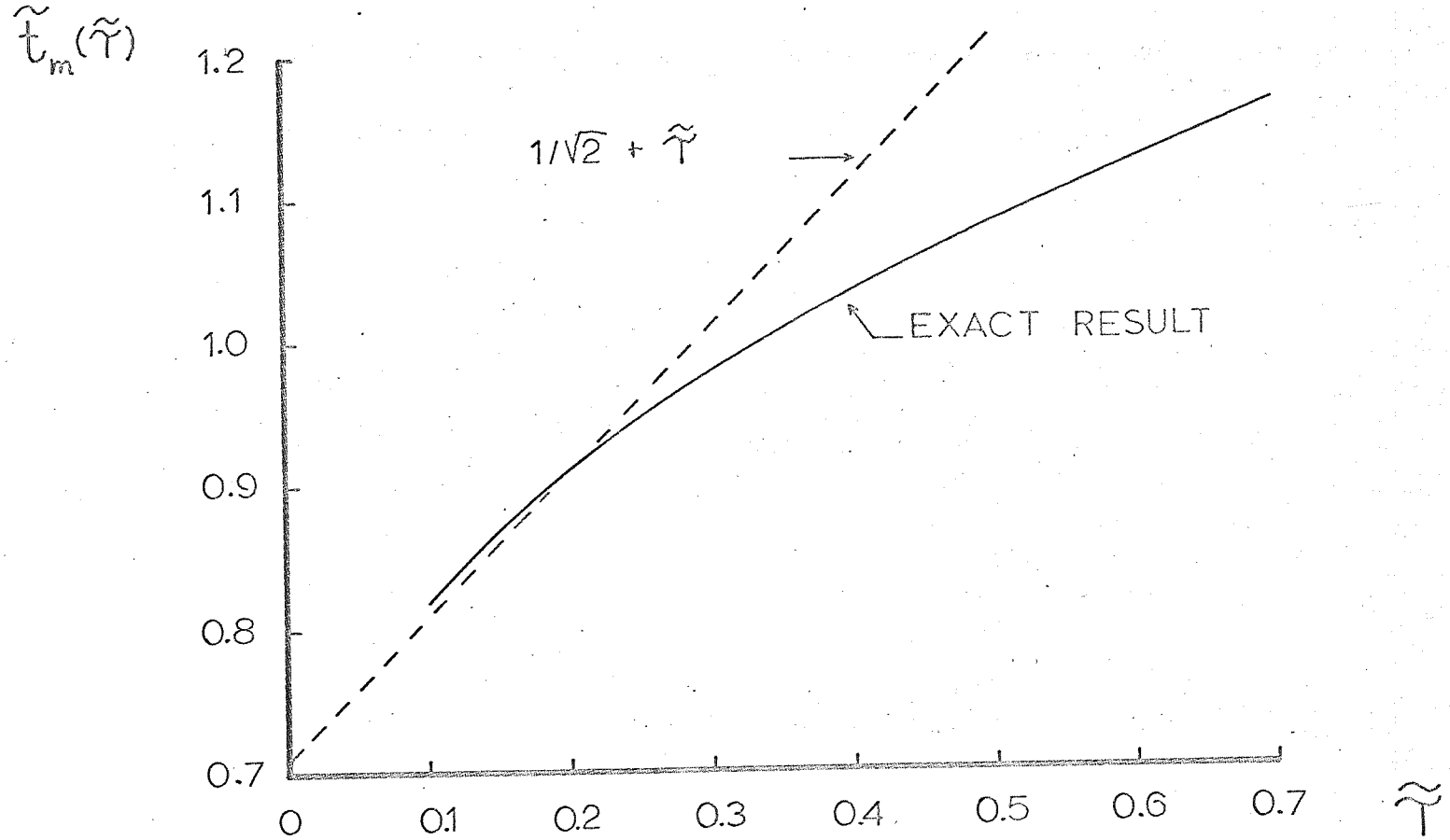

FIGURE 3.3.1 EXACT VALUE OF $\tilde{t}_m(\tilde{\tau})$ AS A FUNCTION OF $\tilde{\tau}$

at time $t = 0$ at the target. Of course this is an idealization, but it is a valid approximation to the real situation if the time required for the slot to pass through the beam is small compared to Δt. The degree to which this assumption is met experimentally is discussed in Chapter V.

CHAPTER IV

EXPERIMENTAL PROCEDURE AND REDUCTION OF DATA

4.1 Procedure

The experimental procedure consisted of the following. With the target holder in place in the test chamber, and the chopper disk rotating at 5000 revolutions per minute, a beam is let into the system by applying test gas pressure to the nozzle stagnation chamber. The detector response is then recorded for the desorption of the test gas from the target at room temperature. The use for this measurement will be discussed in Section 4.2.

After the room temperature reading, the target-holder reservoir is filled with liquid nitrogen. The temperature of the target surface drops slowly enough (for temperatures below about 105 degree Kelvin) that recordings of detector signal can be taken at various temperatures as the target is cooling. When the target temperature reaches its terminal value, heater coils under the target face are used to increase the surface temperature. The heaters, used in conjunction with the cooling effect of the liquid nitrogen, allow the temperature of the target surface to be held constant at various temperatures, and repeat readings are taken to check those made while the target temperature is decreasing.

4.2 Reduction of Data

Typical detector signals are displayed in Figure 3.1.2. The beginning of a pulse is signaled by the photopulse peak at the start of the trace. The value of t_m is obtained in the following way. A smooth curve is faired through the steps of the educted trace at the photopulse and in the vicinity of the response maximum. The maxima of these smooth curves are then selected by taking the point equidistant from the sloping portions of the curve on either side of the maximum. The length (along the horizontal axis) between the maximum of the photopulse and the maximum of the response is then measured and converted to time by means of a length-time conversion factor. This length of time is the uncorrected value of t_m.

Two corrections must be applied to the value of t_m obtained by the aforementioned method. The first of these is a correction for the error in the photopulse timing signal due primarily to the fact that the light beam and molecular beam axes are not exactly 180° out of phase for the chopper. The effect on t_m of this misalignment is dependent on the speed of the chopper. For a fixed chopper speed, the error is equal but opposite in sign depending on the direction of rotation of the chopper. Thus, a correction can be determined by educting two detector signals under identical conditions but with the chopper direction reversed for the second reading. The correction is then

simply half the shift in the value of t_m from the first to the second trace.

The second correction consists of subtracting from the uncorrected value of t_m (corrected for chopper misalignment) the time δ required for the center of the beam pulse to travel from the chopper slot to the target surface. δ is constant for a given gas at a given value of the beam stagnation temperature. δ is obtained from the value of t_m for the target at room temperature as follows. At room temperature, the mean stay time of molecules on the target surface is several orders of magnitude below the stay times we wish to measure, although still long enough for thermal accommodation. Thus, the beam can be considered to strike the target and be reflected diffusely with a Maxwellian distribution of speeds corresponding to room temperature. The time required for a response maximum under these conditions is $\delta + \beta_R L/\sqrt{2}$ where β_R is the value of β at room temperature. It follows that:

$$\delta = (t_m)_{\text{ROOM TEMP}} - \beta_R L/\sqrt{2} \qquad (4.2.1)$$

Thus, the value of t_m consistent with our previous definition (Section 3.3.2) of time zero as the time at which the pulse strikes the surface is obtained by subtracting δ from the uncorrected t_m.

Equation (3.3.8) can now be used to find the mean stay time. For a fixed value of target temperature, $\beta L/\sqrt{2}$ is computed, the corrected value of t_m is obtained as described above and τ thus determined.

CHAPTER V

RESULTS

5.1 Results

Three gases (argon, carbon dioxide, nitrogen) were used with the stainless steel target. The results for carbon dioxide and nitrogen are less substantial than those for argon and will be considered first. Mean stay times measured for nitrogen are shown in Figure 5.1.1; stay times for CO_2 are shown in Figure 5.1.2. It is not the intention of the author to represent these results as being of quantitative value. The scatter in the data is simply too great. However, it is indicated that stay times of the order of 10^{-5} seconds may be present for the range of temperatures shown and that by lowering the target temperature this stay time does appear to increase. Certainly, further experimentation with these two gases is indicated before any quantitative conclusions regarding these data might be made. The remaining discussion in this chapter will be understood to apply to the results for argon.

Mean stay times of argon adsorbing on the present stainless steel target are given in Figure 5.1.3. The stay times show an increasing trend with decreasing temperature. Stay times of the order of 10^{-4} seconds were measured for temperatures below about 85°K. Error flags shown are for

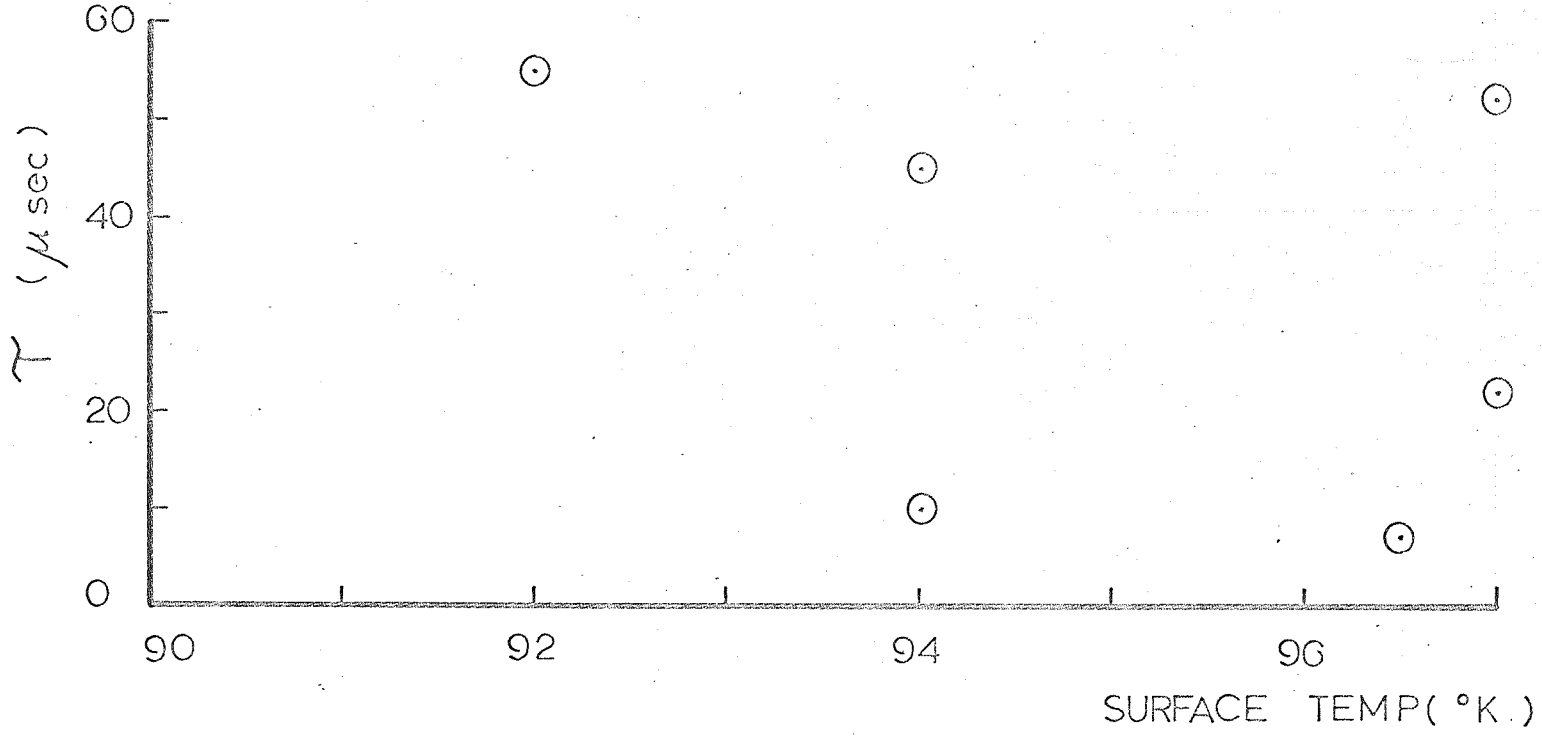

FIGURE 5.1.1
MEAN STAY TIME OF NITROGEN ON STAINLESS STEEL

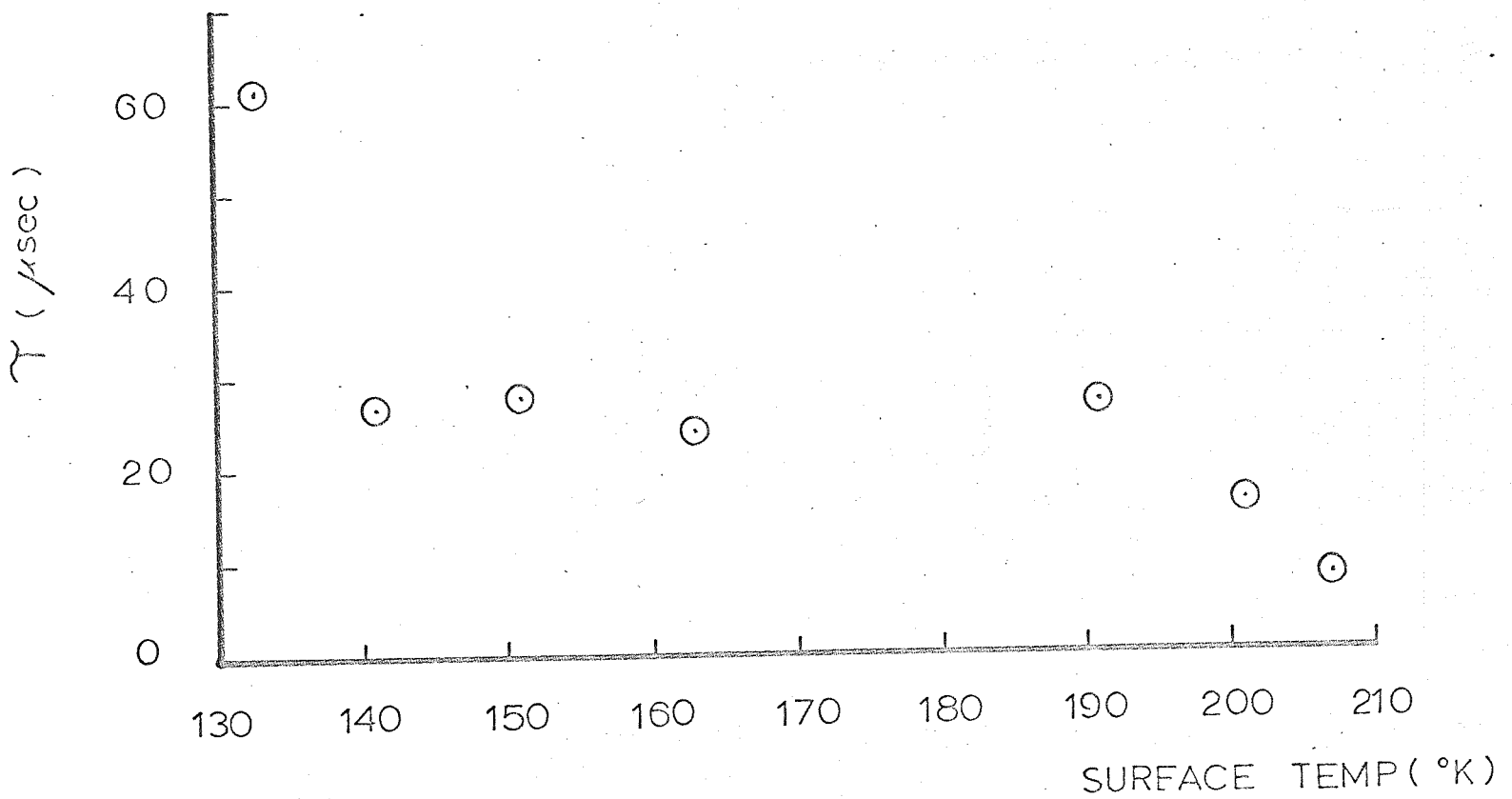

FIGURE 5.1.2
MEAN STAY TIME OF CO_2 ON STAINLESS STEEL

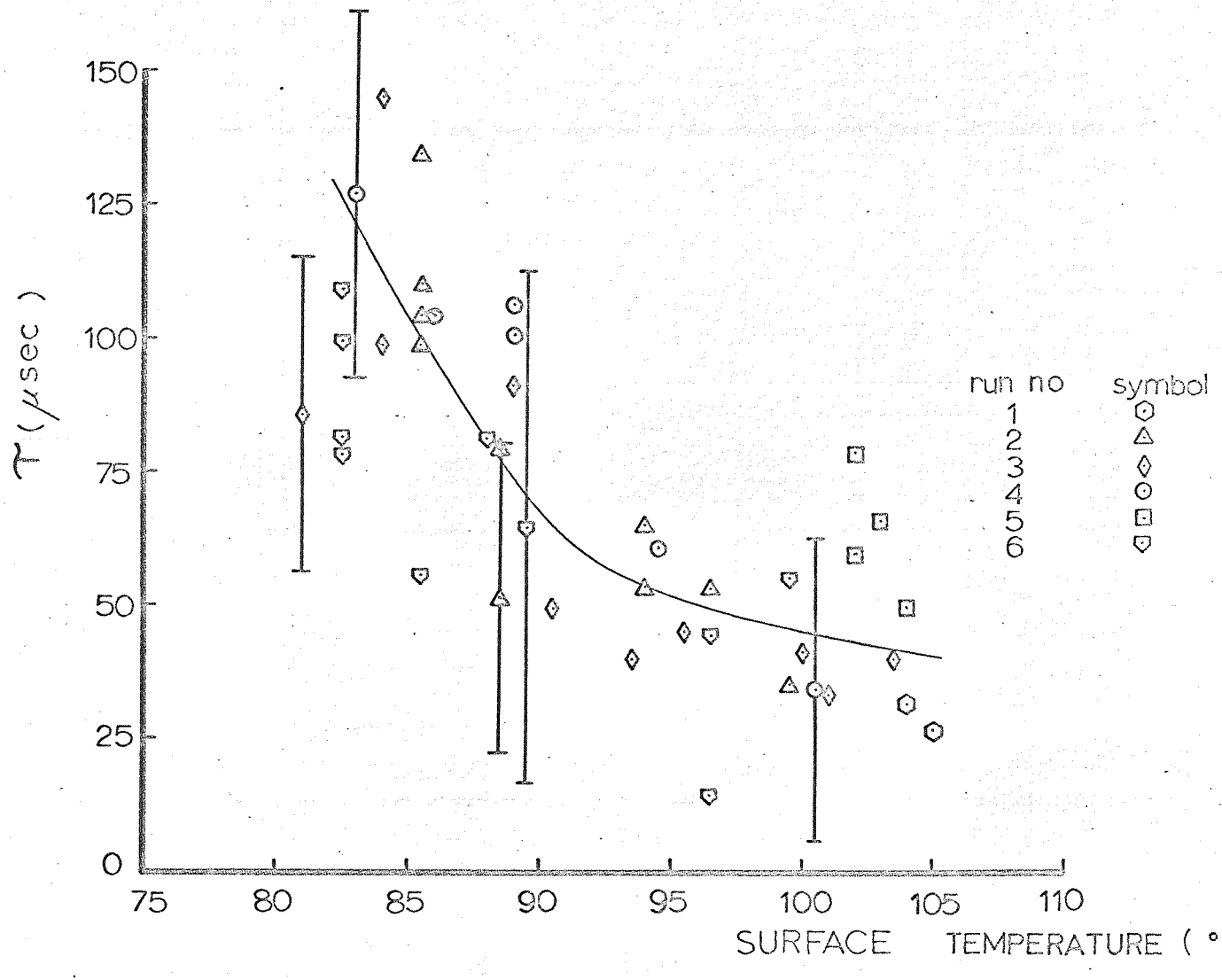

FIGURE 5.1.3 MEAN STAY TIME OF ARGON ON STAINLESS STEEL

outside limit estimates of uncertainties (See Appendix IV). The stay time data for argon can be used to estimate the value of the heat of adsorption for argon on this test surface. Using a value of τ of 50 μsec at a temperature of 95°K indicated by Figure 5.1.3, and assuming a value for τ_o of 2 X 10^{-13} seconds (Section 2.5.1) the value of the heat of adsorption is calculated by Equation (1.2.9) to be 3.7 k cal/mole, in good agreement with estimates given in Section 2.5.1. However, if log τ is plotted as a function of $\frac{1}{T}$ for this data, and a slope is inferred from the plotted points to obtain U and τ_o, the results are entirely different. Figure 5.1.4 is such a plot. The two solid vertical lines indicate the range of measured values of τ at temperatures of 82.5°K and 100°K. The two dashed lines have the minimum and maximum slopes that can be inferred from the data. The range of values of τ_o and U indicated by the slopes and intercepts of these lines is:

τ_o: between 1.7 X 10^{-8} and 1.5 X 10^{-5} sec

U: between 1.50 and 0.28 Kcal/mole

The lack of agreement between these values and expected ones is presumably an indication of two things. First, at higher temperatures (lower 1/T), the slope of the stay-time curve is deformed (slope diminished) by a resolution or small systematic error limitation which caused stay times larger than actual to be indicated. Second, at temperatures below about 85°K the heat of adsorption decreases (due to a

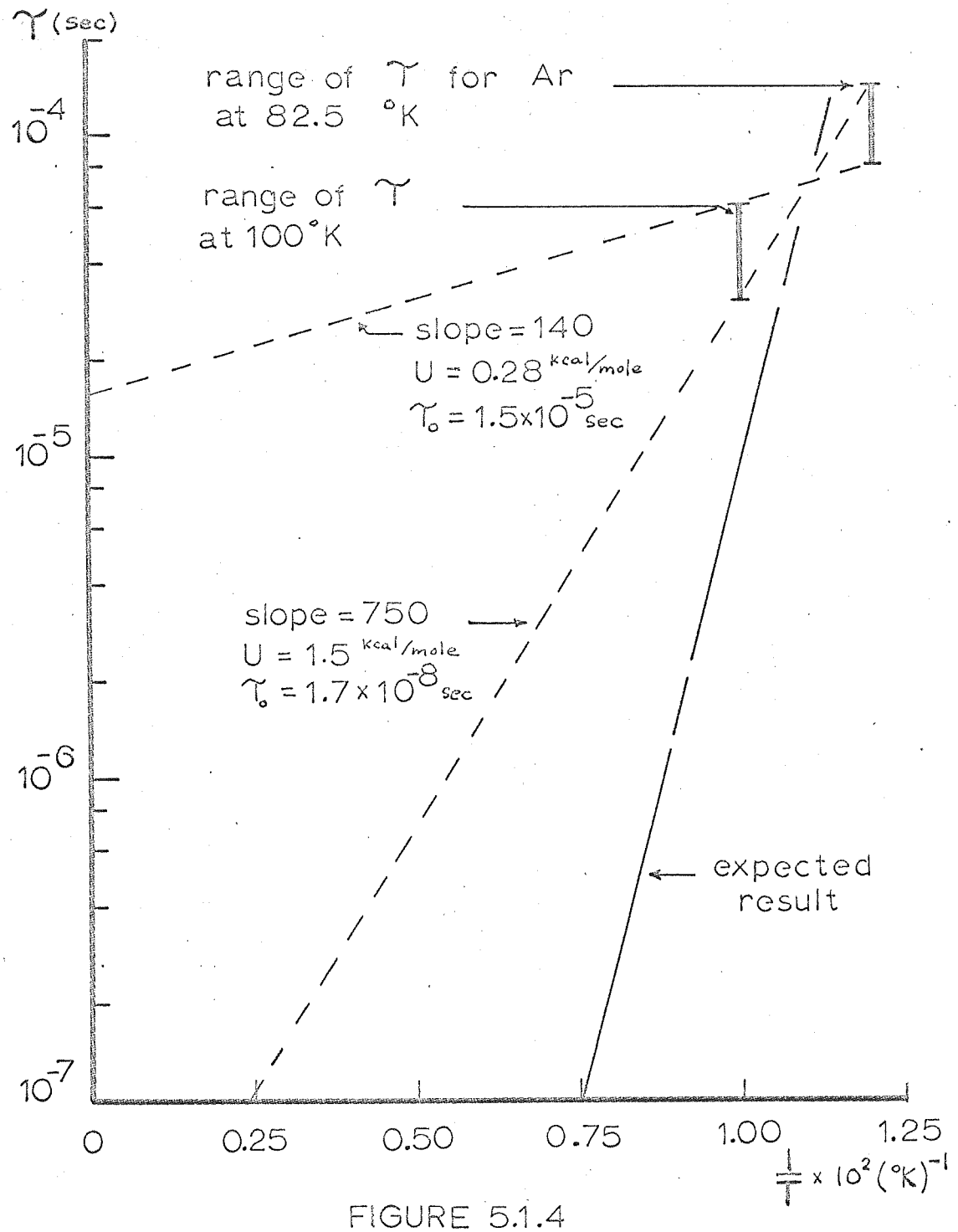

FIGURE 5.1.4
ESTIMATION OF τ_0 AND U FOR ARGON ON STAINLESS STEEL

coverage-dependence effect discussed in Section 5.2) rapidly as the temperature is lowered, again diminishing the slope of the stay-time curve. By comparison, the broken line shown in this figure is the expected variation of τ with 1/T if τ_o were taken as a more reasonable value (2×10^{-13} sec) and U were taken as 3.6 K cal/mole to make this line pass through the center of the data.

5.2 Limitations of the Data

In Figure 5.1.3 the run numbers indicate runs made on different days over a period of several weeks. The argon results, although having a large amount of scatter, are reproducible over day to day experiments within the uncertainty of the measurement (see Appendix IV). This uncertainty is primarily the result of noise in the detector signal leading to an uncertainty in the position of the response maximum as plotted by the chart recorder, and hence an uncertainty in t_m.

In Figure 5.1.3 the values of τ shown are calculated by use of Equation (3.3.8) which is only approximately correct. Figure 3.3.2 shows that the error in this approximate equation increases with $\tilde{\tilde{\tau}}$. Since L, the target-detector traverse length, is a constant in this experiment, the value of $\tilde{\tau}$ depends only upon the dimensional stay time and the target temperature. For the lowest target temperatures and greatest stay times achieved for the argon

experiment, the approximate formula underestimates the value of the stay time by slightly less than 10 per cent. The correction which could be applied to the argon stay times to account for this error is not large enough at the temperatures and stay times of the experiment to be significant when compared with the large uncertainty in the measurement due to noise in the detector signal.

At lower temperatures the following anomaly was exhibited by the argon data. At a given temperature, when successive measurements of the stay time were made at five-minute intervals, the measured stay time decreased for each successive reading. Data exhibiting this phenomenon are shown in Figure 5.2.1. Insufficient data have been obtained to be able to identify the exact temperature where this effect begins to occur. Only two tests were conducted, one at 82.5°K, at which the effect was present, and another at 85.5°K where it was not.

Before considering an explanation of this effect, consider conditions in the test chamber. The target, a surface of machine roughness, is (in addition to the molecular beam) subjected to an atmosphere of 10^{-7} torr. Principal constituents of this background atmosphere are water vapor, nitrogen or carbon monoxide and diffusion pump oil vapor, all of which will undoubtedly adsorb on the target surface at these temperatures. Thus the layer of adsorbate on the surface consists, in part, of a combination of all these

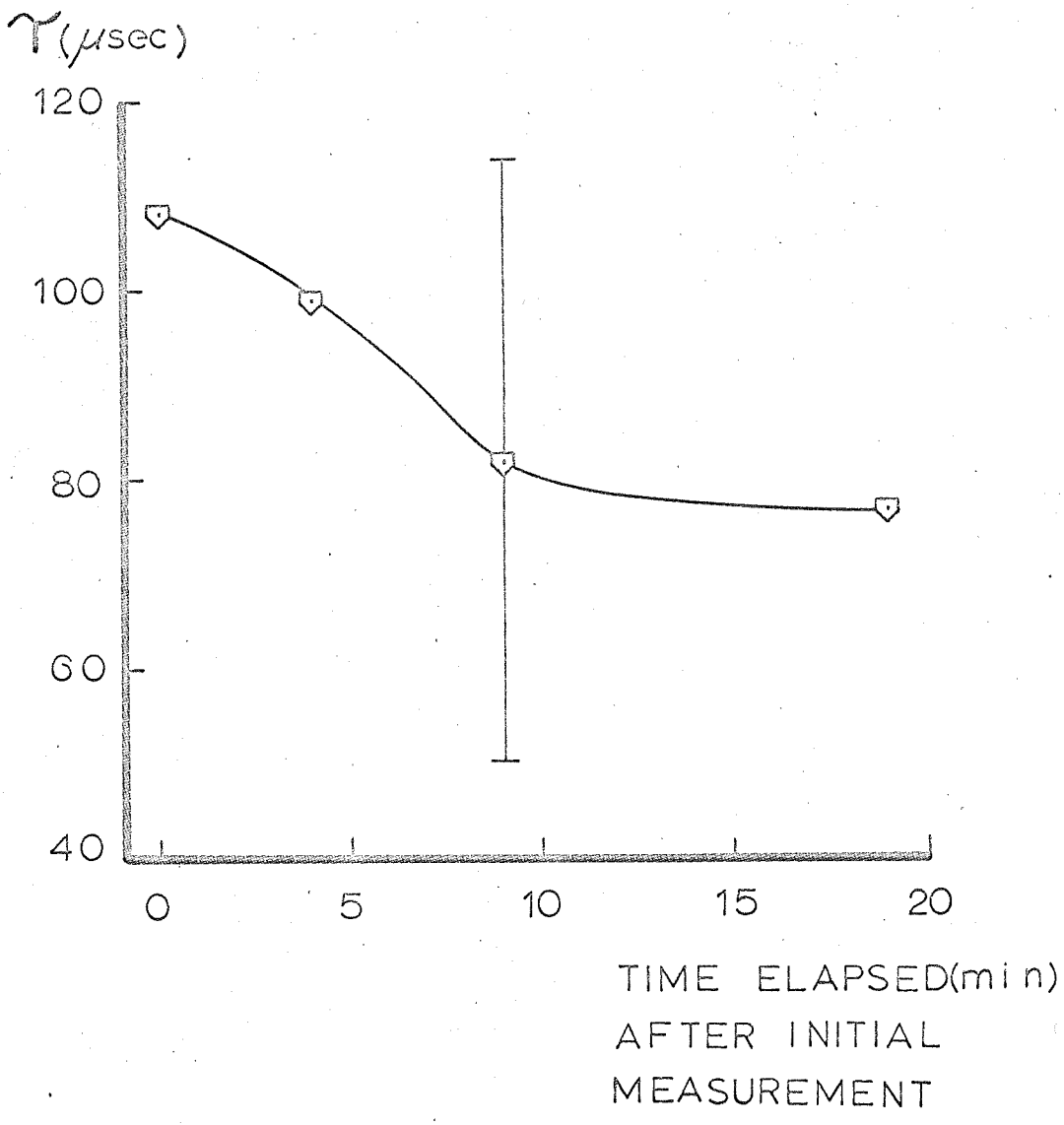

FIGURE 5.2.1 TIME DEPENDENCE OF τ FOR Ar ON STAINLESS STEEL AT A CONSTANT TARGET TEMP. (82.5 °K)

constituents as well as the argon atoms. Insofar as their total or individual coverage is some appreciable fraction of a monolayer, these other gases will affect the argon adsorption.

Returning now to the time-dependent effect mentioned above, the following alternate possibilities are advanced:

a) At higher temperatures in the range of experimental measurements, the non-argon adsorbate remains relatively constant for the more permanently adsorbed gases. This would be the case for saturated coverage of chemisorbed constituents and physisorbed gases such as water vapor. Below about 85°K, however, the nature of this saturation with respect to one or more background atmospheric constituents is altered and a new higher saturation level is approached.* However, since the coverage is time dependent, this implies[5] that the mean stay time corresponding to this new level is large compared to the time of the experiment.

b) Below 85°K, the fractional monolayer coverage of some of the background constituents (most likely those lower molecular weight pump oil vapors which are not efficiently trapped in this range) becomes

*For example, this might correspond to a phase change of some adsorbed constituent, or the beginning of multilayer adsorption.

sufficiently large to have a significant effect on the nature of the argon adsorption. Again, the time dependence must imply that these constituents have mean stay times which are large compared to the time of the experiment.

In order to bypass this time-dependence effect at lower surface temperatures, the following experiment was carried out. Carbon dioxide was bled into the test chamber in sufficient quantity to raise the total background pressure from 10^{-7} to 10^{-6} torr. This insured that the flux of CO_2 molecules onto the target surface was an order of magnitude greater than the total flux of all other background gases. Since CO_2 should continually condense on the surface at these temperatures, the composition of the surface layer seen by the argon beam should be almost totally CO_2 and should be independent of time. This then should eliminate the time dependence due to the adsorption of background gases. Of course, this method completely changes the nature of the surface, and the stay-time results should not be expected to correlate with those for the steel surface. In fact, the heat of adsorption of argon on CO_2 proved too small to be measurable within the resolution of these experiments.

It was stated in Section 3.3.2 that the time duration halfwidth Δt_p of the incident beam pulse should be much less than the time duration halfwidth Δt of the detector response. This is required because a finite value of Δt_p distorts the detector signal from the form predicted by the analysis of Section 3.3.1. Let the time-of-flight resolution $\mathcal{R}$ be defined:

$$\mathcal{R} \equiv \frac{\Delta t}{\Delta t_p} \qquad (5.2.1)$$

In this experiment, with the target at room temperature, $\mathcal{R} \geq 12$. Furthermore, as the target temperature decreased, Δt increased approximately as the inverse square root of the temperature, while Δt_p was held constant. According to Hagena and Varma[10], the distortion of the signal, as measured by a percentage change in Δt, is less than 1 per cent for $\mathcal{R} \geq 12$.

Due to symmetry, for fixed $\mathcal{R}$, the percentage displacement of t_m will be approximately an order of magnitude less than the percentage increase in Δt. Thus, even though the measured values of τ here are small compared to t_m (0.01 t_m to 0.2 t_m), the condition $\mathcal{R} \geq 12$ should assure that there is insignificant error induced in τ due to finite time-of-flight resolution. That is, $\mathcal{R} \geq 12$ should insure that the distortion of τ is less than 0.001 t_m.

CHAPTER VI

CONCLUSIONS

The time-of-flight method described herein appears to be feasible for the measurement of adsorption stay times. The resolution limitation apparent from the initial results, however, indicates that the method would be more suitable for the measurement of somewhat longer stay times. In fact, longer stay times were anticipated, but the effect of the undetermined combination of several more or less permanently adsorbed gases on the stainless steel surface was to diminish the heat of adsorption, and thus the stay time, significantly.

Furthermore, these initial measurements demonstrate the inadequacy of conducting stay-time experiments on a surface whose nature is dependent on time if valid estimates of τ_o and the heat of adsorption are to be deduced from the data. The method of deposition of CO_2 on the target surface for the elimination of time-dependence does not appear to be feasible for argon on CO_2, at least not at the temperatures of this experiment. Possibly this method would produce better results, that is, longer stay times, at lower target temperatures such as might be obtained with some method of cooling other than liquid nitrogen.

Guided by the above findings the following is offered as a possible improvement on the time-of-flight experiment.

1. Use a clean target surface such as might be obtained by vapor-depositing a metal on a substrate in a vacuum.
2. Maintain the clean nature of the surface by operating at much lower background pressures than the 10^{-7} level of this experiment.
3. Provide a means of cooling the target to much lower temperatures than that of liquid nitrogen.

BIBLIOGRAPHY

1. Hartnett, J. P., "A Survey of Thermal Accommodation Coefficients," Rarefied Gas Dynamics, Supplement 1, 1 (1961) (from Advances in Applied Mechanics), Academic Press, New York.

2. Chambre', P. L. and Schaaf, S. A., Flow of Rarefied Gases, Princeton University Press, Princeton, New Jersey, 1961.

3. Langmuir, Irving, "The Evaporation Condensation and Reflection of Molecules and the Mechanism of Adsorption," Phys. Rev., Vol. 8, No. 4, 149, (1916).

4. Frenkel, J., "Theory of Adsorption and Related Phenomena," Z. Physik, Vol. 26, 117, (1924) (English translation, SLA Translation Center, Chicago, Illinois).

5. Clausing, P., "Measurement of the Time of Stay by Experimentation," Physica, Vol. 8, 289 (1929).

6. de Boer, J. H., The Dynamical Character of Adsorption, Oxford University Press, London, 1953.

7. Brunauer, S., The Adsorption of Gases and Vapors, Vol. I Princeton Univ.Press,Princeton,N.J., 1945-(refers to Clausing,P. Ann.der Phys, Vol,5,No. 7, 489,521 (1930).

8. Leonas, V. B., "Study of Energy Transfer During the Collision of a Molecular Stream with a Surface," Zhurnal Prikladnoi Mekhanilci i Tekhnicheskoi Fiziki, No. 2, 84, (1965) (English Translation).

9. Fisher, S. S., Hagena, O. F., and Wilmoth, R. G., "Flux and Speed Distributions of Molecular Beams after Scattering by Metal Surfaces," J. Chem. Phys., Vol. 49, No. 4, 1562, (1968).

10. Hagena, O. F. and Varma, A. K., "Time-of-Flight Velocity Analysis of Atomic and Molecular Beams," Rev. Sci. Instr., Vol. 39, No. 1, 47 (1968).

BIBLIOGRAPHY (continued)

11. Hagena, O. F., Scott, J. E. Jr., and Varma, A. K., Design and Performance of an Aerodynamic Molecular Beam and Beam Detection System," NASA Technical Report, Report No. AST-4038-103-67U, June 1967.

APPENDIX I

DERIVATION OF THE DETECTOR DENSITY FUNCTION

Consider a box of molecules with number density n_o and temperature T, having an orifice with elemental area dA. Let a detector element, subtending a solid angle $d\Omega$, lie at a distance L from the center of the orifice (Fig. A1.1), and let the line of sight along L make angle Θ with the normal to the orifice. Let:

N_t = the number of particles crossing the plane of the imaginary target orifice.

$\frac{d^4N_t}{dAdtd\Omega dv}$ = the number of particles crossing the orifice plane per unit area, per unit time, having speeds within dv about v and paths within $d\Omega$.

Now let f(v) be the number of molecules per unit volume in the box having speeds within dv centered on v. Furthermore, we will eventually let f(v) be the Maxwellian speed distribution:

$$f(v) = \frac{n_o}{(\pi)^{3/2}} \beta^3 v^2 \exp(-\beta^2 v^2) \qquad (A1.1)$$

Now, it follows from the definition of f(v) that

$$\frac{d^4N_t}{dAdtd\Omega dv} = v f(v) \cos\Theta \qquad (A1.2)$$

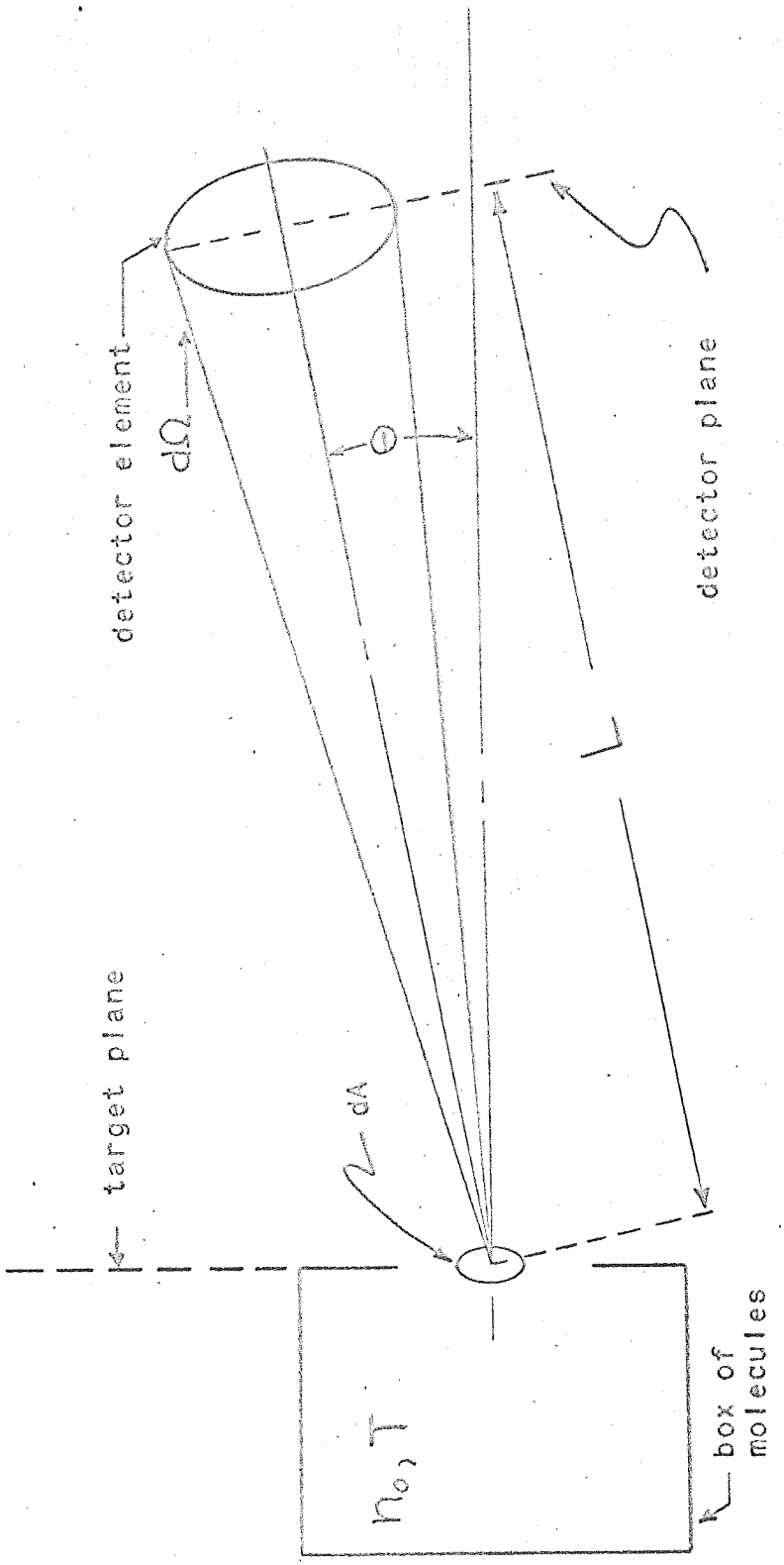

FIGURE A1.1 COORDINATE SYSTEM FOR TARGET AND DETECTOR

For convenience, let us define

$\tilde{N}_t$ = the number crossing per unit time, per unit area, per unit solid angle.

Then:

$$\frac{d\tilde{N}_t}{dv} = vf(v)\cos\Theta \qquad (A1.3)$$

and, integrating formally with respect to v,

$$\tilde{N}_t = \cos\Theta \int_0^\infty vf(v)dv \qquad (A1.4)$$

Before proceeding, first consider a pulse of N particles of infinitesimal time duration leaving the target orifice at $t=t'$. A particle in this pulse having a speed v will reach the detector in time $(t - t') = L/v$. These N particles will arrive at a rate $\frac{dN}{dt}$ at the detector such that:

$$\int_0^\infty \left(\frac{dN}{dt}\right) d(t-t') = N \qquad (A1.5)$$

It follows that the particles making up the pulse $\tilde{N}_t dt'$ which depart the surface within time interval dt' at t' will be distributed in arrival rate at the detector according to:

$$\frac{d}{dt}\left(\tilde{N}_t dt'\right) = \frac{d}{dt}\left[\cos\Theta \int_0^\infty v f(v)\, dv \;\; dt'\right]$$

$$= \cos\Theta\left(\frac{L}{t-t'}\right) f\left(\frac{L}{t-t'}\right) \left|\frac{dv}{dt}\right| dt'$$

$$= \frac{\cos\Theta}{L}\left(\frac{L}{t-t'}\right)^3 f\left(\frac{L}{t-t'}\right) dt' \qquad \text{(A1.6)}$$

The total arrival rate of particles arriving at the detector at time t is obtained by integrating over the range of t', all of A_t, and for all Ω subtended by the detector, say, Ω_d. Let us call this arrival rate $\frac{dN_d}{dt}$. Then:

$$\frac{dN_d}{dt}(t) = \int_{t'} \int_{A_t} \int_{\Omega_d} \frac{\cos\Theta}{L}\left(\frac{L}{t-t'}\right)^3 f\left(\frac{L}{t-t'}\right) d\Omega\, dA\, dt' \qquad \text{(A1.7)}$$

To the extent that A_t and Ω_d are suitably small, Eq. (A1.7) may be integrated over Ω and A with the integrand held constant. Thus:

$$\frac{dN_d}{dt}(t) \doteq A_t \Omega_d \int_{t'} \frac{\cos\Theta}{L}\left(\frac{L}{t-t'}\right)^3 f\left(\frac{L}{t-t'}\right) dt' \qquad \text{(A1.8)}$$

Suppose now that the target is provided with a shutter that opens to allow particles to depart only during the interval t'_o to $t'_o + \delta t'_o$. Furthermore, let us assume $(t-t'_o) >> \delta t'_o$, that is, we are interested in the detector response long after the shutter closes. It follows for this t that $f(L/t-t')$ is slowly varying

with t' in the range $(t'_o) \leq t' \leq (t'_o + \delta t'_o)$, and therefore, Eq. (A.1.8) integrates directly to give:

$$\frac{dN_d}{dt}(t) \doteq \delta t'_o \, A_t \, \Omega_d \, \frac{\cos}{L} \left(\frac{L}{t-t'_o}\right)^3 f\left(\frac{L}{t-t'_o}\right) \tag{A1.9}$$

Finally, since $(t-t'_o) >> \delta t'_o$, all particles arriving at time t will have speeds approximately equal to v, and thus, the density of particles at the detector, $n_d(t,t'_o)$, will be:

$$n_d(t,t'_o) \doteq \frac{dN_d}{dt} \cdot \frac{1}{v(t) A_d} \tag{A1.10}$$

where $A_d = \Omega_d L^2$

and $v(t) = L/(t-t'_o)$ (A1.11)

Therefore:

$$n_d(t,t'_o) \doteq \frac{\delta t'_o \, A_t \cos\Theta}{L^3} \left(\frac{L}{t-t'_o}\right)^2 f\left(\frac{L}{t-t'_o}\right) \tag{A1.12}$$

Substituting for f ($v = L/t-t'_o$) from Eq. (A1.1) and, for simplicity, dropping the zero subscript on t'_o and the approximate equality notation:

$$n_d(t,t') = \frac{\delta t' A_t \cos\Theta}{L^3} \cdot \frac{n_o \beta^3}{(\pi)^{3/2}} \left(\frac{L}{t-t'}\right)^4 \exp\left[-\beta^2 L^2/(t-t')^2\right] \tag{A1.13}$$

$$n_d(t,t') = n_o \, \delta t' \, C \, (t-t')^{-4} \exp\left[-\beta^2 L^2/(t-t')^2\right] \qquad \text{(A.1.14)}$$

where $$C = \frac{A_t \beta^3 L \cos\Theta}{\pi^{3/2}} \qquad \text{(A.1.15)}$$

Eq. (A.1.14) is equivalent to Eq.(3.3.1) of the text.

APPENDIX II

MAXIMUM OF THE DETECTOR RESPONSE FOR $\tilde{\tau} \ll 1$

The response of the detector is proportional to the integral (see Eq. 3.3.6):

$$G = \int_0^{\tilde{t}} \exp\left(-\frac{\tilde{t}'}{\tilde{\tau}}\right) \exp\left[-(\tilde{t}-\tilde{t}')^{-2}\right] (\tilde{t}-\tilde{t}')^{-4}\, d\tilde{t}' \tag{A2.1}$$

where all times are nondimensionalized with respect to βL . We wish to find the value of $\tilde{t}$ for which the detector response is a maximum. Since the detector response is merely a constant multiplier of G , this is equivalent to finding the value $\tilde{t}_m(\tilde{\tau})$ for which G in Eq.(A2.1) is a maximum. Now if $\tilde{\tau}$ is much less than $\tilde{t}_m(\tilde{\tau})$, then as $\tilde{t}'$ varies from 0 to $\tilde{t}$ in the integration, $\exp(-\tilde{t}'/\tilde{\tau})$ approaches zero much more rapidly than the quantity $(\tilde{t}-\tilde{t}')^{-4}\exp\left[-(\tilde{t}-\tilde{t}')^{-2}\right]$. That is, $\exp(-\tilde{t}'/\tilde{\tau})$ goes from unity to zero while $(\tilde{t}-\tilde{t}')^{-4}\exp\left[-(\tilde{t}-\tilde{t}')^{-2}\right]$ is essentially equal to $\tilde{t}^{-4}\exp(-\tilde{t}^{-2})$. This means that, for $\tilde{\tau} \ll \tilde{t}$, the integral G may be evaluated using approximations based on $\tilde{t}'/\tilde{t} \ll 1$.

To obtain the value of $\tilde{t}$ for which G is a maximum, take $\frac{dG}{d\tilde{t}}$ using Leibnitz' rule, and set $\frac{dG}{d\tilde{t}}=0$ at $\tilde{t} = \tilde{t}_m(\tilde{\tau})$:

$$\frac{dG}{d\tilde{t}}\left[\tilde{t}_m(\tilde{\tau})\right] = \int_0^{\tilde{t}_m(\tilde{\tau})} \exp\left(-\frac{\tilde{t}'}{\tilde{\tau}}\right)\left\{\exp\left[-(\tilde{t}-\tilde{t}')^{-2}\right](\tilde{t}-\tilde{t}')^{-4}\right\}\left\{\frac{2}{(\tilde{t}-\tilde{t}')^3}-\frac{4}{(\tilde{t}-\tilde{t}')}\right\} dt' = 0 \tag{A2.2}$$

For $\tilde{t}'/\tilde{t} << 1$, the terms in the integrand can be expanded in powers of $\tilde{t}'/\tilde{t}$, and, after neglecting terms quadratic and higher in $\tilde{t}'/\tilde{t}$, the integral (A2.2) becomes

$$0 = \int_0^{\tilde{t}_m(\tilde{\tau})} \exp\left(-\frac{\tilde{t}'}{\tilde{\tau}}\right) \left\{\left[\exp\left(-\frac{1}{\tilde{t}^2}\right)\frac{1}{\tilde{t}^4}\right]\left[\left(1-2\frac{\tilde{t}'}{\tilde{t}^3}\right)\left(1+4\frac{\tilde{t}'}{\tilde{t}}\right)\right]\right\}$$

$$\times \left\{\frac{2}{\tilde{t}^3}\left[1+3\frac{\tilde{t}'}{\tilde{t}}\right] - \frac{4}{\tilde{t}}\left[1+\frac{\tilde{t}'}{\tilde{t}}\right]\right\} d\tilde{t}' \qquad \text{(A2.3)}$$

Performing the indicated multiplication, and again neglecting terms of order $(\tilde{t}'/\tilde{t})^2$, we obtain, after some rearrangement:

$$0 = \int_0^{\tilde{t}_m(\tilde{\tau})} \exp\left(-\frac{\tilde{t}'}{\tilde{\tau}}\right)\left\{1-2\tilde{t}^2-\left[10\tilde{t}^2-11+\frac{2}{\tilde{t}^2}\right]\frac{\tilde{t}'}{\tilde{t}}\right\} d\tilde{t}' \qquad \text{(A2.4)}$$

Eq. (A2.4) can be readily integrated to obtain:

$$1-2\tilde{t}_m^2(\tilde{\tau})-\left[10\,\tilde{t}_m^2(\tilde{\tau})-11+\frac{2}{\tilde{t}_m^2(\tilde{\tau})}\right]\frac{\tilde{\tau}}{\tilde{t}_m(\tilde{\tau})} = 0 \qquad \text{(A2.5)}$$

We expect that

$$\tilde{t}_m(\tilde{\tau}) = \tilde{t}_m(0)\left[1+F\left\{\frac{\tilde{\tau}}{\tilde{t}_m(0)}\right\}\right] \qquad \text{(A2.6)}$$

where, consistent with our original assumption of $\tilde{\tau} << 1$, F (which represents the shift in $\tilde{t}_m$ due to $\tilde{\tau}$) will be small compared to one. Using Eq. (A2.6) in Eq. (A2.5) and

neglecting terms quadratic in F, we obtain:

$$2F - [11 - 5(1+2F) - 4(1-2F)] \frac{\tilde{\tau}}{\tilde{t}_{m(0)}} = 0 \qquad (A2.7)$$

Solving Eq. (A2.7) for F, we find:

$$F = \frac{\frac{\tilde{\tau}}{\tilde{t}_{m(0)}}}{1 + \frac{\tilde{\tau}}{\tilde{t}_{m(0)}}} \doteq \frac{\tilde{\tau}}{\tilde{t}_{m(0)}} \qquad (A2.8)$$

Finally, substituting for F in Eq. (A2.6) we obtain:

$$\tilde{t}_m(\tilde{\tau}) = \tilde{t}_m(0) + \tilde{\tau} \qquad (A2.9)$$

It may be easily shown that $\tilde{t}_m(0) = 1/\sqrt{2}$, so

$$\tilde{t}_m(\tilde{\tau}) = \frac{1}{\sqrt{2}} + \tilde{\tau} \qquad (A2.10)$$

or, in dimensional form:

$$t_m(\tau) = \frac{\beta L}{\sqrt{2}} + \tau \qquad (A2.11)$$

APPENDIX III

NUMERICAL EVALUATION OF $\tilde{t}_m(\tilde{\tau})$

It is required to find the value of $\tilde{t}$ for which the integral

$$G = \int_0^{\tilde{t}} (\tilde{t}-\tilde{t}')^{-4} \exp\left[-\frac{\tilde{t}'}{\tilde{\tau}} - (\tilde{t}-\tilde{t}')^{-2}\right] d\tilde{t}' \qquad \text{(A3.1)}$$

is a maximum. To do this, let the interval of integration (0 to $\tilde{t}$) be broken up into n equal intervals $\Delta\tilde{t}'_i$. Let the integrand, $I(\tilde{t}'_i, \tilde{\tau})$ be evaluated at the center, $\tilde{t}'_i$, of each interval $\Delta\tilde{t}'_i$. Holding $\tilde{\tau}$ constant, the integral is evaluated by the sum:

$$G \doteq \sum_{i=0}^{n} I(\tilde{t}'_i, \tilde{\tau}) \cdot \Delta\tilde{t}'_i \qquad \text{(A3.2)}$$

This step is then repeated for another value of $\tilde{t}$ and another, et cetera until the value of $\tilde{t}$ is found for which G is a maximum. This value is $\tilde{t}_m(\tilde{\tau})$. This process in turn is repeated for a different value of $\tilde{\tau}$. $\tilde{t}_m(\tilde{\tau})$ can be found to any desired accuracy (given sufficient computing time) simply by making the intervals $\Delta\tilde{t}'_i$ sufficiently small (n sufficiently large) and by taking

the successive trial values of $\tilde{t}$ sufficiently close together. These computations were carried out on a Burroughs B5500 computer taking n = 100, and later, taking n = 1000. n = 1000 is considered to be a large enough number for the accuracy desired in this analysis for the following reason. The value of $\tilde{t}_m$ ($\tilde{\tau}$) found by taking n = 1000 changed slightly (less than 0.3%) from those obtained with n = 100. Furthermore, in the case of n = 1000, the trial increments of $\tilde{t}$ were typically = .005 $\tilde{t}_m$ ($\tilde{\tau}$). Therefore the accuracy of determination of $\tilde{t}_m$ ($\tilde{\tau}$) as a function of $\tilde{\tau}$ as shown in Figure 3.3.1 is about 99.5%.

APPENDIX IV

ESTIMATION OF UNCERTAINTIES

As explained in Section 4.2, the corrected value of $t_m(\tau)$ is obtained from the measured value of $t_m(\tau)$ by subtracting a correction δ :

$$[t_m(\tau)]_c = [t_m(\tau)]_M - \delta \qquad \text{(A4.1)}$$

where the subscripts c and M denote corrected and measured values respectively. Remember that for a given geometry and chopper motor speed, δ = constant. Now according to the analysis of Section 3.3.2 and Appendix II , for $\tau << t_m(\tau)$ (which applies to the bulk of the data),

$$[t_m(\tau)]_c \doteq \beta L/\sqrt{2} + \tau \qquad \text{(A4.2)}$$

Combining Eqs. (A4.1) and (A4.2) and solving for τ :

$$\tau \doteq [t_m(\tau)]_M - \delta - \beta L/\sqrt{2} \qquad \text{(A4.3)}$$

Recall from Section 4.2 that the correction δ, is determined from the following expression:

$$\delta = (t_m)_{M,R} - \beta_R L/\sqrt{2} \qquad \text{(A4.4)}$$

where $(t_m)_{M,R}$ is measured for a room temperature target and β_R is the value of β for a room temperature target. Using Eqs. (A4.4) in (A4.3), we obtain:

$$\tau = \left[t_m(\tau) \right]_M - (t_m)_{M,R} + \frac{\beta_R L}{\sqrt{2}} - \frac{\beta L}{\sqrt{2}} \qquad \text{(A4.5)}$$

Since both values of t_m in Eq. (A4.5) are now understood to be measured values, let us adopt a more compact notation:

$$\left[t_m(\tau) \right]_M = t_m(\tau)$$

$$(t_m)_{M,R} = t_{m,R}$$

Now writing $\beta = \left(\frac{m}{2kT} \right)^{\frac{1}{2}}$ and $\beta_R = \left(\frac{m}{2kT_R} \right)^{\frac{1}{2}}$ in Eq. (A4.5) we have:

$$\tau = t_m(\tau) - t_{m,R} + A L \left(\frac{1}{\sqrt{T_R}} - \frac{1}{\sqrt{T}} \right) \qquad \text{(A4.6)}$$

where $A = \left(\frac{m}{2k} \right)^{\frac{1}{2}}$.

Now consider the uncertainty $\Delta\tau$ in the mean stay time as a result of uncertainties ΔT, ΔT_R, $\Delta t_m(\tau)$ Δt_{mR}, and ΔL:

$$\pm \Delta\tau = \pm \Delta t_m(\tau) \mp \Delta t_{m,R} \pm A \left(\frac{1}{\sqrt{T_R}} - \frac{1}{\sqrt{T}} \right) \Delta L$$

$$\pm A L \, \Delta \left(\frac{1}{\sqrt{T_R}} - \frac{1}{\sqrt{T}} \right) \qquad \text{(A4.7)}$$

where

$$\pm\Delta\left(\frac{1}{\sqrt{T_R}}-\frac{1}{\sqrt{T}}\right)=\mp\frac{1}{2}\left[\frac{\Delta T_R}{(T_R)^{3/2}}-\frac{\Delta T}{(T)^{3/2}}\right] \qquad (A4.8)$$

Using Eqs. (A4.8) in (A4.7) and taking appropriate signs for the maximum uncertainty we obtain:

$$\Delta\tau=\Delta t_m(\tau)+\Delta t_{m,R}+A\left(\frac{1}{\sqrt{T}}+\frac{1}{\sqrt{T_R}}\right)\Delta L + \frac{AL}{2}\left[\frac{\Delta T}{(T)^{3/2}}+\frac{\Delta T_R}{(T_R)^{3/2}}\right] \qquad (A4.9)$$

Now let us consider the following estimates of uncertainties:

ΔT = 2 ^{o}K (thermocouple measurement)

ΔT_R = 0.5 ^{o}K (precision thermometer measurement)

ΔL = 1 mm (alignment of target)

$\Delta t_{m,R}$ = 9 μsec (half the width of one eductor step)

$t_m(\tau)$ is measured from a noisier signal than $t_{m,R}$, so $\Delta t_m(\tau)$ is estimated by considering the maximum possible influence the signal noise could have in determining the position of $t_m(\tau)$. The estimated values of $\Delta t_m(\tau)$ ranged from 13 to 31 μsec depending on the data sampled. The error flags shown in Fig. 5.1.3 are obtained by using the above estimated uncertainties in Eq. (A4.9). It should be pointed out that $\Delta t_m(\tau)$ and $\Delta t_{m,R}$ account for most of

the uncertainty in Υ .